Competition is a determinant of multidrug resistant plasmid acquisition in *Salmonella*

Running Title: Commensal bacteria can competitively exclude *Salmonella* Heidelberg

Adelumola Oladeinde[1,2,7*], Zaid Abdo[2*], Benjamin Zwirzitz[3,4¶], Reed Woyda[2¶], Steven M. Lakin[2¶], Maximilian O. Press[5¶], Kimberly Cook[6], Nelson A. Cox[1], Jesse C. Thomas IV[7], Torey Looft[8], Michael J. Rothrock[1], Gregory Zock[9], Jodie Plumblee Lawrence[1], Denice Cudnik[1], Casey Ritz[9] and Samuel E. Aggrey[9]

Authors' Affiliation

[1]U.S. National Poultry Research Center, USDA-ARS, Athens, GA, USA. [2]Department of Microbiology, Immunology and Pathology, Colorado State University, Fort Collins, Colorado, USA. [3]Institute of Food Safety, Food Technology and Veterinary Public Health, University of Veterinary Medicine, Vienna, Austria. [4]Austrian Competence Centre for Feed and Food Quality, Safety, and Innovation FFoQSI GmbH, Tulln, Austria.[5]Phase Genomics Inc, Seattle, WA, 98109, USA. [6]Office of National Programs, USDA-ARS, Beltsville, Maryland, USA. [7]Division of STD Prevention, National Center for HIV/AIDS, Viral Hepatitis, STD and TB Prevention, Center for Disease and Control, Atlanta, Georgia, USA. [8]National Animal Disease Center, USDA-ARS, Ames, IA, USA,[9]Poultry Science Dept, University of Georgia, Athens, GA, USA

Corresponding authors* ade.oladeinde@usda.gov; zaid.abdo@colostate.edu

¶ These authors contributed equally to this work.

Abstract

Host microbiome homeostasis ensures that gut conditions are unfavorable to an invading pathogen such as *Salmonella enterica*. Consequently, fostering a "balanced" gut microbiome through the administration of microbes that can competitively exclude pathogens has gained a lot of attention and use in human and animal medicine. However, little is known on how competitive exclusion affects the transfer of antibiotic resistance. To shed more light on this question, we challenged neonatal broiler chicks raised on reused broiler chicken litter – a complex environment comprising of decomposing pine shavings, feces, uric acid, feathers, and feed, with *Salmonella* Heidelberg (S. Heidelberg), a model pathogen. We show that chicks raised on reused litter carried lower abundance of *Salmonella* and harbored a more uniform and diverse microbiome comprising of bacterial species that are known to provide colonization resistance towards *Salmonella* compared to chicks raised on fresh bedding composed of pine shavings. Additionally, these bacterial species were associated with a lower horizontal transfer of multidrug resistance genes to *S*. Heidelberg. Using in vitro competition experiments, we confirmed that conjugation between *S.* Heidelberg and *E. coli* strains from chicks raised on fresh litter resulted in the acquisition of multidrug resistant plasmids. Contrastingly, bacteriophage-mediated recombination between *S*. Heidelberg and *E. coli* strains made the acquisition of plasmid-mediated β-lactamase gene (bla_{CMY-2}) possible. Collectively, this study demonstrates that competitive exclusion can reduce the transfer of antibiotic resistance and provides information on the bacterial species that can be explored for their benefits to reduce antibiotic resistance transfer.

Importance/Significance

Antimicrobial resistance spread is a worldwide health challenge, stemming in large part, from the ability of microorganisms to share their genetic material through horizontal gene transfer. To address this issue, many countries and international organization have adopted a one health approach to curtail the proliferation of antibiotic resistant bacteria. This includes the removal and reduction of antibiotics used in food animal production and the development of alternatives to antibiotics. However, there is still a significant knowledge gap in our understanding of how antimicrobial resistance spreads in the absence of antibiotic selection and the role commensal bacteria play in reducing antibiotic resistance transfer. In this study, we demonstrate that commensal bacteria play a key role in reducing the horizontal transfer of antibiotic resistance to *Salmonella* and provide the identity and characteristics of the bacterial species that performs this function in broiler chickens.

67 # Introduction

68 Horizontal gene transfer is recognized as the main way bacteria acquire antibiotic
69 resistance (AR) and exposure to antibiotics has been shown to be a driver of antibiotic
70 resistance gene (ARG) transfer (1). Consequently, the rise in AR bacteria in hospital
71 settings has been linked to the overuse of antibiotics in humans and its use in food animal
72 production (2, 3). These public health concerns have led to a reduction in antibiotics used
73 for raising food animals (4, 5), including a ban on antibiotics use in Europe (6). However,
74 how much reduction in AR transfer is achievable from removal is still poorly understood.
75 We previously showed that neonatal broiler chicks challenged with a susceptible *S*.
76 Heidelberg (SH) strain and raised antibiotic-free on fresh bedding composed of pine
77 shavings acquired multidrug resistant (MDR) SH strains at a high rate (7). We also
78 demonstrated that horizontal transfer of a MDR plasmid from *E. coli* strains to SH
79 conferred the MDR phenotype (7). We selected SH as the model pathogen because of
80 its promiscuity to plasmids carrying AR (8, 9).

81 There is limited research on if and how competitively exclusion reduces AR in food-
82 borne pathogens (10-16) such as *Salmonella enterica* or the role it plays in AR reduction
83 and transfer. Therefore, the goal of this study was to determine the role competitive
84 exclusion plays in limiting *Salmonella enterica* from acquiring AR and provide information
85 on the bacterial species and mechanism involved. To do this, we compared the dynamics
86 of AR transfer in neonatal broiler chicks raised on fresh bedding composed of pine
87 shavings to chicks raised on reused litter. We chose reused litter because it is a complex
88 environment made up of decomposing plant-based bedding (e.g., wood shavings,
89 sawdust and rice or peanut hulls) mixed with chicken feces, uric acid, feathers, feed,

90 insects, and other broiler-sourced materials. Therefore, reused litter carries a unique and
91 complex population of bacteria, fungi, viruses (17-19), interacting with various forms of
92 eukaryotes, making it a suitable environment to study competitive exclusion. Broiler
93 chickens are commonly raised on litter but how litter is managed differs between
94 countries, producers, and farmers. For instance, the practice of reusing litter over multiple
95 flock of broiler chickens is a widespread practice in the US and Brazil while Canada (20)
96 and European counterparts (21) recommend fresh litter bedding for every flock. One
97 argument against litter reuse is that it harbors pathogenic bacteria that can be horizontally
98 transferred to the next flock (22). Contrastingly, proponents of litter reuse argue it confers
99 competitive exclusion against pathogens when effectively managed and it is cost-effective
100 (23-26). Beyond broiler chicken production, competitive exclusion by "beneficial"
101 microbes has received enormous attention in the 20th century, resulting in the bloom of
102 commercially marketed probiotics (27) and the underlying theory behind the application
103 of fecal microbiota transplantation in human medicine (28).

104 # Results

105 **Neonatal broiler chicks raised on reused litter did not acquire antibiotic resistant**
106 ***S*. Heidelberg**

107 Total *Salmonella* concentration in the ceca of broiler chicks was higher for chicks on fresh
108 litter compared to chicks on reused litter using both culture (p=0.15) and qPCR methods
109 (p = 0.29) (Fig. 1a and b). However, *Salmonella* concentration in the litter was variable
110 and differed between culture and qPCR method. For instance, *Salmonella* was higher in
111 fresh litter compared to reused litter using qPCR (p = 0.34) but higher in reused litter (p =
112 0.08) using culture method. The number of cecal samples positive for *Salmonella* after

113 enrichment in buffered peptone water (BPW) was 76% (n =34) for fresh litter and 63% for
114 reused litter (n =35). Chicks inoculated via the cloaca were all positive for *Salmonella*
115 after ceca was enriched in BPW regardless of the litter type. A few cecal (n = 5) and litter
116 (n = 2) samples from the uninfected control chicks were positive for *Salmonella* with
117 qPCR and after enrichment in BPW. Lastly, 36 % of SH isolates (n = 158) from the ceca
118 and litter of chicks from fresh litter acquired MDR (i.e., resistance to gentamicin,
119 tetracycline, and streptomycin), compared to 0.7 % of the isolates (n =141) from reused
120 litter (Fig. 1e).

121 **Reused litter carried lower abundance of transferable plasmids than fresh litter**

122 We used qPCR to target selected genes present on the MDR IncI1-pMLST26 plasmid
123 that was acquired by SH (7). There was no significant difference in the abundance of
124 IncI1, *aadA* and *tetA* (p>0.2) between fresh and reused litter but reused litter carried lower
125 levels of these genes (Fig. 1c). Class -1 integron gene (*IntI1*) was significantly higher in
126 reused litter compared to fresh litter (p = 0.03). In the ceca, *tetA* (p=0.01) *and aadA*
127 (p=0.04) were higher for chicks on reused litter compared to chicks on fresh litter.

128 To determine the plasmid and ARG types in the ceca, we aligned metagenome
129 assembled contigs of cecal samples (n = 4) to plasmid and ARG reference sequences
130 available on PlasmidFinder and ResFinder databases (see methods for description). This
131 revealed that chicks from fresh litter carried more plasmids (n = 6±4) than chicks on
132 reused litter (n = 3±2), including the MDR IncI1 plasmid that was acquired by SH (7) (Fig.
133 1d). Similarly, the ceca of broiler chicks from reused litter carried fewer ARG contigs (n =
134 2±2) than chicks on fresh litter (n = 16±3). The majority of the ARG's found confer
135 resistance to various drugs in the aminoglycoside class of antibiotics. Together, this data

136 suggests that reused litter harbored fewer MDR plasmids that could be transferred to
137 *Salmonella* compared to fresh litter.

138 **Neonatal chicks raised on reused litter harbored a diverse population of beneficial**
139 **microbes and upregulated metabolic pathways**

140 The alpha diversity of the bacterial community present in the ceca and litter of chicks on
141 reused litter was higher for the observed species measure (Ceca $p<0.001$, litter $p=0.001$)
142 but not for Shannon (Ceca $p=0.25$, litter $p=0.05$) and Simpson (Ceca $p=0.969$, litter
143 $p=0.28$) index (Supplementary Fig. 1a). Chicks on reused litter carried a more uniform
144 bacterial community in their ceca and litter compared to chicks on fresh litter and beta
145 diversity was affected by the route chicks were inoculated with SH (Supplementary Fig.
146 1b and c). Actinobacteria was higher in reused litter compared to fresh litter while
147 Proteobacteria and Bacteroidetes were higher in fresh litter compared to reused litter (Fig.
148 2a; Supplementary Fig. 2). In the ceca, Actinobacteria and Proteobacteria were higher in
149 the ceca of broiler chicks on reused litter compared to chicks on fresh litter. We
150 determined that members of the genus *Bifidobacterium*, *Brevibacterium*,
151 *Brachybacterium*, *Corynebacterium*, *Faecalibacterium*, *Escherichia/Shigella*,
152 *Halomonas, and Salinococcus* among others contributed significantly to the higher
153 diversity of litter and ceca of chicks raised on reused litter compared to fresh litter (Fig.
154 2b).

155 To determine the species associated with the 16S rRNA amplicon sequence variants
156 found in reused litter, we aligned shot gun reads from the ceca of broiler chicks on fresh
157 (n =2) and reused (n = 2) litter (~111 million reads per sample) to Kraken database (30).
158 We identified ten species of *Bifidobacterium* including *B. longum* (21% of the genera),

159 and *B. catenulatum (*11% of the genera*)* that had the most abundant reads in the genus
160 (Fig. 2c; Supplementary File 1 - All supplementary files are available in Dryad repository:
161 https://datadryad.org/stash/share/tRAj54_iZbJ52xnBIakiN0czHPSoXqWcCdAd6FWamv
162 o). *Escherichia/Shigella* were represented by *E. coli* (~98% of the genera, *E. albertii*, *E.*
163 *marmotae*, *E. fergusonii*, *S. dysenteriae*, *S. boydii*, *S. flexneri* and *S. sonnei*.
164 *Faecalibacterium prausnitzii*, *Salinicoccus halodurans and Jeotgalicoccus*
165 *saudimassiliensis* were the only species identified using shot gun reads. We identified
166 between 18 – 59 species for the genera *Halomonas*, *Streptococcus*, *Lactobacillus* and
167 *Corynebacterium* (Supplementary File 1).
168 Next, we used metagenome assembled genomes (MAGs) to assess functional
169 pathways that were enriched in the ceca of chicks from fresh compared to reused litter.
170 The average assembly size and number of contigs was 1,238,395,273±167,820 bp and
171 1,797,423±281253 for the four samples. The number of MAGs found in reused litter was
172 higher (754±409) than fresh litter (156±98). Pathways related to biosynthesis of organic
173 and antimicrobial molecules were enriched to a greater degree in reused litter samples
174 than in fresh litter samples (Fig. 2d). Of note was the enrichment of antimicrobial
175 biosynthesis pathways in reused litter (macrolides, tetracyclines, and carbapenems),
176 suggesting an increased level of competition between bacterial species as the litter
177 became more used. Increased competition in reused litter was supported by a
178 simultaneous increase in molecules that are targets of antimicrobials, such as folate,
179 which is the target of the sulfonamides. Contrastingly, pathways associated with the
180 biosynthesis of secondary metabolites of plants including flavonoids and indole-alkaloids
181 were enriched in samples from fresh litter.

182 **Neonatal chicks raised on reused litter carried fewer MDR *E. coli* strains**

183 Microbiota analyses revealed that SH invasion of the chicken gut resulted in a reduction
184 of *E. coli* populations in the ceca of chicks raised on fresh and reused litter, while the
185 cecal metagenome revealed that *E. coli* was the main reservoir of multidrug resistant IncI1
186 plasmids (7). Furthermore, *E. coli* population was higher for broiler chicks on reused litter
187 compared to chicks on fresh litter (Fig. 3a). Therefore, we retrospectively screened the
188 ceca of broiler chicks from fresh and reused litter for susceptible and multidrug resistance
189 *E. coli* strains and sequenced the genomes of nineteen selected strains.
190 We observed that the phylogeny of the *E. coli* strains could be explained by the litter
191 used for raising broiler chicks. For instance, phylogroups A, D and F were only found in
192 the ceca of chicks raised on fresh litter, whereas phylogroups B1 were restricted to the
193 ceca of chicks from reused litter, except for one strain that belonged to phylogroup A (Fig.
194 3b and c). Likewise, multi locus sequence type (MLST) classification showed that ST 69,
195 2705 and 6858 were associated with *E. coli* strains originating from fresh litter. The only
196 ARG carried by *E. coli* strains from reused litter was bla_{TEM-1B}, except for one MDR isolate.
197 On the other hand, *E. coli* strains from fresh litter harbored multiple ARG on their
198 chromosome and plasmids, including the MDR IncI1 plasmid that was acquired by SH.

199 **Competition experiments between SH and *E. coli* strains resulted in the acquisition**
200 **of MDR IncI1 plasmids.**

201 To confirm the transfer of MDR plasmids from *E. coli* to SH and to determine the
202 mechanism involved, we performed a competition experiment on solid CHROMagar™
203 with an antibiotic susceptible SH strain and four *E. coli* strains (n = 2 *E. coli* strains from
204 fresh and reused litter, respectively) that differed in their virulence and AR genes (Fig.4a,

205 Supplementary File 2). To decipher the role of transduction (bacteriophage-mediated
206 transfer) in MDR acquisition, we added either Ca^{2+} to CHROMagar™, a cation required
207 for phage adsorption to bacterial cells, or citrate which chelates Ca^{2+} (31). Additionally,
208 we used synthetic 2-hexadecynoic acid (2-HDA), a potent inhibitor of conjugal plasmid
209 transfer (32) to determine if cell-to-cell contact (conjugation) was needed for MDR plasmid
210 transfer from *E. coli* to SH (Fig. 4a).

211 Adding citrate to CHROMagar™ reduced the population of SH (X^2=13.03, df =3, P =
212 0.004) and *E. coli* (X^2=19.83, df =3, P = 0.0002) and SH did not acquire MDR (Fig. 4b
213 and c). However, SH acquired gentamicin (gen^R) and ampicillin (amp^R) resistance in the
214 absence of citrate, 2-HDA and $CaCl_2$. Gentamicin resistant SH population appeared at a
215 lower a rate when 2-HDA was added to CHROMagar™ compared to controls (X^2=15.71,
216 df =3, P = 0.001) (Fig. 4b). We observed a 24 h delay in the appearance of amp^R SH and
217 colony counts did not follow the expected dilution-fold differences or were too numerous
218 to count (n = 9) (Supplementary Fig. 3a). Furthermore, none of the amp^R SH isolates (n
219 = 9) selected from $CaCl_2$ plates were resistant to ampicillin after a second susceptibility
220 screen. For amp^R isolates that passed the second screen, 8 of 35 displayed AmpC β-
221 lactamase resistance phenotype by broth microdilution (these eight ampR isolates are
222 thereafter referred to as amp^R recombinants) while 13 were resistant to cefoxitin. This
223 suggested that amp^R was not stable in SH after acquisition.

224 To determine the genetic determinants associated with amp^R and gen^R, we
225 sequenced nineteen SH recombinants including susceptible isolates. Amp^R recombinants
226 harbored IncI1-pMLST12 (pST12) encoding bla_{CMY-2}, whereas gen^R recombinants carried
227 IncI1-pMLST26 encoding multidrug resistance. In addition, SH recombinants that

228 acquired pST12 lost parental resistance to nalidixic acid. It is noteworthy to mention that
229 none of the *E. coli* strains harbored pST12 or bla_{CMY-2} and suggests that recombination
230 of genes caused an emergence of pST12.

231 **The acquisition of IncI1 plasmid carrying bla_{CMY-2} gene altered the genome of *S.***
232 **Heidelberg**.

233 To determine the HGT mechanism involved in the emergence and transfer of pST12, we
234 compared mutations found in gen^R to amp^R recombinants. Amp^R recombinants had
235 parallel/hotspot mutations in 107 loci on the chromosome and 3 loci on IncX1 plasmid
236 (Supplementary File 3). A KEGG orthology analysis examining proteins affected by these
237 mutations suggests they are involved in enzyme metabolism, amino acid and secondary
238 transport, and transcription of DNA to RNA (Supplementary Table 1). In addition, 20%
239 (18 of 87) of proteins affected by mutations are associated with P22 bacteriophage
240 infection (33) (Supplementary File 3). For instance, we found mutations in genes that are
241 part of an O-antigen gene cluster (*rfbBCP)*. The *rfb* cluster genes are either required for
242 or aid in P22 infection (33). Surprisingly, the *gyrA* mutation that conferred nal resistance
243 was reverted in all amp^R recombinants. In comparison, we did not find *gyrA* reversion or
244 hot spot mutations in gen^R or susceptible recombinants, but all recombinants carried 6
245 mutations in the intergenic region between P4-like prophage DNA-binding transcriptional
246 regulator AlpA (Supplementary Table 2) and virulence factor PgtE. Furthermore, the
247 MLST (34) of the core genome of amp^R recombinants (cgST=114049) differed from that
248 of the ancestor (cgST=171516) and genR or susceptible recombinants (cgST=186980).

249 A ML tree with chromosomal SNPs and accessory genes (Fig. 5a and b) grouped
250 amp^R recombinants on the same clade with agar lysate and distantly separated them from

251 gen^R and/or susceptible recombinants. Furthermore, a whole genome alignment with
252 protein sequences of two complete chromosomal contigs showed that inversion occurred
253 in the amp^R recombinant and not in gen^R recombinant (Supplementary Fig. 4). This
254 inversion affected a 700 Kbp region and deletions in the intergenic regions of 5S-23S and
255 5S-16S rRNA gene contributed to *oriC* reorientation.

256 The clustered regularly interspaced short palindromic repeats (CRISPRs) and their
257 associated cas immunological system is supposed to supply memory of the foreign
258 genetic elements that have invaded the host bacteria. In SH, there are two CRISPR I-E
259 systems (CRISPR1 and 2) known to perform this function (35). Therefore, we compared
260 the CRISPR-Cas genes in SH recombinants to determine if acquisition of protospacers
261 associated with CRISPR adaptation occurred. We found a 305-bp CRISPR repeat in
262 CRISPR2 for all amp^R recombinants that was absent in gen^R recombinants or the SH
263 ancestor (Supplementary Fig. 5a and d). This included 5 direct-repeats (29 bp each)
264 interspersed by 5 spacers (32 bp) – hereafter referred to as spacer 1 – 5. The extra
265 repeats were inserted between spacer 3 and repeat 4 of the ancestral CRISPR2
266 (Supplementary Fig. 5a). Furthermore, the extra repeat had higher DNA sequence
267 coverage than the surrounding CRISPR2 DNA sequence (n = 7, V = 28, P = 0.015)
268 (Supplementary Fig. 5b).

269 To decipher the biogenesis of this repeat, we performed BLAST alignment against
270 the genome of *E. coli* donors. We reasoned that SH could add spacers against non-self-
271 foreign DNA. We found regions of homology in the repeat region of all *E. coli* donors, but
272 no homology was found for the spacers (Supplementary Fig. 5c). To determine the targets
273 of the spacers, we performed searches against curated phage, plasmid and transposon

274 databases using NCBI or CRISPRtarget (36). We found no match for spacer 1, 3 and 5,
275 albeit spacer 2 matched IncFIB plasmids present in *Raoultella Orthinolytica* (RefSeq:
276 NZ_CP012557.1) and *Pantoea* sp. (RefSeq: NZ_CP022519) and spacer 4 matched
277 CRISPR2 spacers in several *S*. Heidelberg and *S*. Typhimurium genomes. The matching
278 spacer 2 was found in a ParB/RepB/Spo0J family plasmid partition protein (SopB)
279 encoded by Inc (F4: A-: B1) (59 % pairwise DNA identity i.e., 19 of 32 bases were 100%
280 identical) and IncI1 plasmids (pST12 and pSTnovel are 52% identical to spacer 2) present
281 in *E. coli* donor strains from fresh litter (Supplementary Fig. 5d and e). These results
282 suggested that acquisition of IncI1 plasmid carrying bla_{CMY-2} gene changed the genome
283 and sequence type of SH recombinants.

284 **Identifying how a bacteriophage facilitated the transfer of IncI1 plasmid carrying**
285 **bla_{CMY-2} gene**

286 Compared to conjugation, transduction is more likely to lead to a change in bacterial gene
287 content, genetic structure, and mutations. To determine if a bacteriophage mediated
288 pST12 transfer, we sequenced the lysate extracted from citrate treated CHROMagar™
289 and performed long read sequencing on a gen^R and amp^R recombinant to achieve
290 complete genomes. For amp^R recombinant, complete circular contigs were assembled
291 for IncX1 and ColpVC plasmid, while the longest chromosomal contig measured 4.7Mb
292 (Supplementary Table 3). The rest of the contigs were determined to be part of pST12
293 (~101 kb). Contrastingly, the gen^R recombinant assembly resulted in a complete
294 chromosome, IncX1 and Col8282 and the remaining contigs were mapped to pMLST26
295 (~107 kb).

296 Next, we aligned the sequence reads of the lysate to SH genome and de-novo
297 assembled the unmapped reads. Our hypothesis was that SH transcription would be
298 directed towards transducing phage proteins and therefore would have greater number
299 of sequenced read coverage. After read alignment, we found a ~40 kb CDS region
300 encoding *Salmonella* P22 phage with twice the coverage of the SH chromosome
301 (Supplementary Fig. 6; supplementary figures 6-13 are available in Dryad repository:
302 https://datadryad.org/stash/share/tRAj54_iZbJ52xnBIakiN0czHPSoXqWcCdAd6FWamv
303 o). Additionally, the assembled unmapped reads were pST12, suggesting the lysate
304 carried a transducing particle (Supplementary Table 3). Furthermore, SH strains that
305 acquired pST12 carried mutations affecting P22 including a mutation downstream of *gtrC*
306 (serotype conversion gene) and phage tail (endorhamnosidase) (Supplementary File 3).
307 To determine how the pST12 plasmid backbone evolved, we performed multiple
308 alignment of all chromosome and plasmid contigs from *E. coli* donors except IncX1
309 (present in the SH, thus incompatible) and Col plasmids and used pST12 contigs as the
310 reference genome (Fig. 5c). This revealed that pST12 was a chimera of plasmids and
311 chromosomal genes with a pST26 and novel IncI1 (pSTnovel) backbone (pST12 is ~40%
312 identical to pMLST26 and ~30% to pSTnovel). Other plasmids that were determined to
313 be part of pST12 were *inc* groups FIB/FII and IncHI1B/p0111. For example, *inc*FIB/FII
314 present in Ec-RL-1X was the only plasmid harboring the five uncharacterized genes
315 located between *ccdA* and *cia*, and no plasmid was identified for regions encoding *ISEc9-*
316 *sugE-blc-amp*C.
317 After comparing the pST12 from this study with identical plasmids (n = 93), we found
318 only twenty-four genes to make up its core genome. These included genes encoding

319 conjugal transfer (*tra, dot and icm)* and tyrosine recombinase *(xerD)*. (Supplementary
320 Table 4). A ML tree reconstructed with accessory genes revealed that the closest MLST
321 to pST12 comprised of non-typeable plasmids, ST24, ST26 and ST36 (Supplementary
322 Fig. 7). Furthermore, a KEGG orthology analysis of the IncI1 plasmids from this study
323 revealed they share gene modules for secretion system, cytoskeleton, and prokaryotic
324 defense system, but pST26 and pST12 have additional modules for transport and AR
325 (Supplementary Table 5). These results suggest that recombination between plasmids
326 and chromosomal genes present in strains of *E. coli* and SH gave rise to IncI1 plasmid
327 carrying bla_{CMY-2} gene and a P22 bacteriophage aided its transfer to SH.

328 **Identifying recombination events between SH and *E. coli* that gave rise to a**
329 **transferable bla_{CMY-2} gene.**

330 We found an AmpC region with identical DNA sequences to bla_{CMY-2} on the
331 chromosome of *E. coli* and SH. This region encodes translation elongation factor (*efP*),
332 quaternary ammonium compound-resistance (*sugE),* outer membrane lipoprotein (*blc*),
333 AmpC β-lactamase (*blaMIR)* and fumarase reductase genes (*frdABCD*) in *E. coli*, but in
334 SH a *luxR* regulator and an uncharacterized protein replaced AmpC. A phylogenetic tree
335 built with the AmpC/Frd operon showed that *E. coli* donors (Ec-FL-1X and Ec-FL-2X) were
336 the closest relative (78%) to the bla_{CMY-2} region in pST12 (Supplementary Fig. 8). The *frd*
337 proteins of SH and *E. coli* (*frd* of SH is 87 % identical to *frd* of *E. coli*) are more closely
338 related compared to *blc-sugE (blc-sugE* of SH is 70% identical to *blc-SugE* of *E. coli)*.
339 The results suggested that AmpC was mobilized from the chromosome to IncI1.

340 We did not find the *ISEc9* transposon that was co-mobilized with AmpC in *E. coli*
341 donor strains or SH recipient but *ISEc9* was present on the chromosome of agar lysate

342 and amp^R recombinants (Supplementary Fig. 9a). *ISEc9* was inserted into the
343 chromosome of amp^R recombinants, and it truncated an uncharacterized protein (*ynfC*)
344 located downstream of spermidine N (1)-acetyltransferase (*speG*) (Supplementary Fig.
345 8). Similarly, *ISEc9* was inserted into a hypothetical protein (*yagA*) in pST12 and in so
346 doing truncated the *yagA* gene (Supplementary Fig. 9b). This suggested that *ISEc9* was
347 first encoded on the chromosome before it was mobilized to IncI1. A BLAST search
348 against the NCBI RefSeq database revealed that multiple chromosomal regions in
349 *Enterobacteriaceae* encode *ISEc9* (n= 50) including *Salmonella* (n = 19) and *E. coli* (n
350 =9). For ~ 60% of the occurrences, bla_{CTX-M} or bla_{CMY-2} was the neighboring gene to *ISEc9*
351 (Supplementary File 4). For example, *S*. Typhimurium strains (Genbank: CP022062 and
352 CP028314) carried *ISEc9* and bla_{CMY-2} on their chromosome and on a IncI1 plasmid.
353 In *E. coli*, the promoter of *ampC* overlaps *frdD* and serves as a transcriptional
354 terminator of the Frd operon. Therefore, AmpC and Frd operon are tightly coupled and
355 changes in the overlapping region are expected to affect both operons (37). The Frd
356 operon is important for anaerobic respiration and requirement for fumarate can drive the
357 transcription of a cascade of genes (38) and lead to the formation of antibiotic resistant
358 bacterial persisters (39). This selection for fumarate may explain the reports of plasmids
359 encoding Frd and AmpC operon in *Enterobacteriaceae* species (39-41). We searched the
360 cecal metagenomes for pST12 and found contigs with identical protein sequences (n
361 =119, mean contig size = 7,858 bp, smallest contig = 1,000 bp, largest contig = 103,724
362 bp) including a ~ 18 kb contig encoding AmpC/Frd operon in chicks from fresh litter
363 (Supplementary Fig. 9a ; Supplementary File 5). Likewise, we found contigs matching
364 pST12 (n =121, mean contig size = 22,643 bp, smallest contig = 1,017 bp, largest contig

365 = 243,272 bp) in the cecal metagenome of chicks from reused litter and one contig (~18
366 kb) also carried AmpC/Frd operon. We did not find any contig encoding *ISEc9* in the cecal
367 metagenome but when we restricted our BLAST search to viral genomes available on
368 NCBI, we found *ISEc9* on two bacteriophages - *Enterobacter* phage LAU1 and
369 *Salmonella* phage SJ46.

370 *E. coli* donor strains carried multiple lambda phages and SJ46 (Supplementary Fig.
371 11a) and some shared proteins with significant homology with P22 phage in SH. For
372 instance, donor Ec-FL-1X harbored two lambda phages with one encoding lysozyme R
373 (*rrrD*), superinfection exclusion protein B (*sieB*) and recombination proteins (*ninBE*)
374 (Supplementary Fig. 11b). These genes are important for bacterial host lysis, resistance
375 to phage re-infection and phage recombination, and their presence suggests P22 can
376 lysogenize the *E. coli* genomes used in this study and vice versa. Similarly, P22 encodes
377 two regions of homology with pSTnovel, including its coat protein (~9% identical to *parA*
378 in pSTnovel) that is required for P22 packaging and Rha family transcriptional regulator
379 (~12% identical to *repZ* in pSTnovel). Together, our results suggest that selection for
380 fumarate genes encoded by *E. coli* and SH gave rise to recombinants carrying bla_{CMY-2}
381 on an IncI1 plasmid, and bacteriophages aided its mobilization from chromosome to
382 plasmid.

383 **Proposing a transduction model for IncI1 plasmid carrying bla_{CMY-2} gene**

384 Competition resulted in the lysis of some *E. coli* and SH strains and our model suggests
385 that P22 erroneously acquired part of their genome during procapsid packaging and
386 transduced this DNA after re-infecting SH (Supplementary Fig. 12a). P22 can transduce
387 DNA that are between 2- 5% of the size of its genome i.e., < 750 - 2,000 bp (42). Further,

388 DNA regions in multiple copies and under selection are expected to be transduced at a
389 higher rate than low copy DNA (43, 44). In this study, we determined this region to encode
390 AmpC/Frd operon in *E. coli* donors. We could not identify the origin of *ISEc9* transposon
391 or why it is co-located with *blc-sugE*-AmpC in IncI1, but our results suggest it was formed
392 during transduction. By inserting itself next to *speG*, an indispensable protein for
393 polyamine detoxification, *ISEc9* was maintained in the chromosome and transferred to a
394 plasmid by a bacteriophage.

395 Amp^R recombinants carried a high copy small ColpVC plasmid and an IncX1 with 3
396 hotspot mutations including a 22-bp iteron deletion. When we compared the hotspot
397 mutations of amp^R recombinants to other SH genomes carrying ColpVC, we found that
398 all genomes carried 50 and 3 hotspot mutations on their chromosome and IncX1,
399 respectively (Supplementary File 6; Supplementary Fig. 12b). In our previous work (45),
400 we demonstrated that SH strains that had a deleted iteron carried a higher copy of IncX1,
401 which we speculated was needed for mobilizing ColE1 plasmids. This was also true in
402 this study, Amp^R recombinants carried higher copies of IncX1 (1.81 ± 0.05 copies per cell)
403 than gen^R and susceptible recombinants (1.16 ± 0.17 copies per cell) ($W = 0$, $P < 0.001$).

404 The non-coding region downstream of the origin of replication of ColpVC (84 bp) is
405 94% identical to the origin of transfer (*oriT*) of the relaxosome (*nikA*) of pST12 and
406 pSTnovel (~ 110 bp region upstream of *nikA*). In addition, we found the region upstream
407 of *nikA* to have the highest sequence coverage (8X for pST12 and 5X for pSTnovel) when
408 compared to the rest of the IncI1 genomes (Supplementary Fig. 12c). Likewise, ColpVC
409 had the highest genome coverage (~13,000X) (Supplementary Fig. 12c) and the
410 chromosomal region encoding P22 had twice the coverage of the chromosome

411 (Supplementary Fig. 6). This suggests that IncI1 and P22 bacteriophages are capable of
412 mobilizing ColpVC plasmids.

413 It is plausible that carriage of ColpVC provides conjugative plasmids with extra *oriT*
414 that is required for conjugation, while ensuring their own mobilization. Consequently,
415 encapsulation of ColpVC by bacteriophages not only enhances the stability of ColpVC
416 but also helps maintain IncI1 plasmids in the bacterial host. Indeed, early studies on P22
417 transduction suggested that P22 infection aids productive rolling circle replication of
418 ColE1 plasmids by providing a substrate for headful packaging (43). The 2.2kb size of
419 ColpVC puts it in the upper end of the predicted genome size P22 can transduce. There
420 is no reported benefit ColpVC gives the bacterial host, but it is prevalent in SH strains
421 harboring IncX1 and/or pST12 (9). Rodriguez-Rubio et al (44) showed that encapsulation
422 of multicopy Col plasmids by bacteriophages increased AR transfer 10,000-fold
423 compared to encapsulation of low copy plasmids.

424 **Discussion**

425 Establishing a "balanced" gut microbiome through the administration of probiotics has
426 gained a lot of attention and use in human and animal medicine, but its effect on AR
427 transfer is not fully understood. Casaburi et al (46) showed that infants fed a probiotic
428 strain of *Bifidobacterium longum* exhibited a change in their gut microbiome, resulting in
429 a 90 % lower level of ARG compared to non-fed controls. In this study, we show that
430 commensal bacterial populations from reused broiler chicken litter provided colonization
431 resistance against the conjugal transfer of multidrug resistant plasmid to *S*. Heidelberg
432 present in the gut of neonatal chicks. We identified several bacterial species from the
433 genera *Bifidobacterium*, *Faecalibacterium, Corynebacterium* and *Escherichia* to be

434 involved in the competitive exclusion of antibiotic resistant *Salmonella* and determined
435 the metabolic pathways used. Though we measured only two cross-sectional timepoints
436 for reused and fresh litter, the relative abundance of plant-metabolic related pathways in
437 fresh litter compared to the enrichment of competitive molecules in reused litter suggests
438 that a selective pressure gradient exists over time for the colonizing microbial populations
439 in reused litter. Together, these characteristics suggests that reused litter is a highly
440 competitive environment for *Salmonella* to successfully colonize.

441 Although neonatal chicks raised on reused litter did not acquire MDR S. Heidelberg,
442 our analysis of the cecal metagenome and whole genome sequencing of *E. coli* strains
443 originating from reused litter confirmed that transferable plasmids were indeed present in
444 reused litter. Additionally, a competition experiment involving *E. coli* strains from fresh
445 and reused litter suggested that selection for fumarate encoding genes led to the
446 development of β-lactam resistant *S*. Heidelberg populations and not antibiotic selection.
447 The ampC/frd region is part of a large mobile genomic island-like (~140kb) chromosome
448 region encoding P4 bacteriophage in some *Enterobacteriaceae* species (47). We
449 confirmed the location of the island in one of the *E. coli* donor strain from fresh litter
450 (Supplementary Fig. 13). The mobility of this region following *E. coli* lysis was key to the
451 emergence and transfer of the most reported (48, 49) plasmid-mediated AmpC β-
452 lactamase gene (bla_{CMY-2}) gene to *S*. Heidelberg in our study.

453 The vertebrate host uses multiple defense mechanisms to protect the gut against an
454 invading pathogen including its microbiome. The microbiome competes with pathogens
455 for space and nutrients, and through this process confers colonization resistance against
456 an invader. Consequently, the microbiome regulates a variety of host immune responses

457 and has been demonstrated to shape the gut-brain communication (50, 51). This
458 communication between the host and its microbiome ensures that gut conditions are
459 unfavorable to a pathogen such as *Salmonella*. This can be achieved by reducing the
460 stomach pH and oxygen levels to levels that only favor short chain fatty acid producers
461 (52) and oxygen-sensitive bacterial species (53) including members of the phylum
462 Firmicutes. However, some strains/serotypes of non-typhoidal *Salmonella enterica* have
463 developed mechanisms to evade the host microbiome-imposed colonization resistance.
464 Through evolution, these strains have acquired repertoire of genes for acid resistance
465 and anaerobic metabolism. Furthermore, *Salmonella* has been shown to modulate the
466 microbiome present in the gut of broiler and layer chickens after challenge with
467 *Salmonella* Enteritidis or Typhimurium (52, 54).

468 Pathogen induced gut modulation can create an imbalance in the abundance of
469 bacterial species i.e., some species outgrow known resident bacteria, leading to a
470 dysbiosis of the gut microbiome and successful *Salmonella* colonization and antibiotic
471 transfer (55, 56). In this study, we observed that competition from commensal bacteria in
472 reused litter significantly reduced *S*. Heidelberg population that acquired AR from *E. coli*
473 strains harbored by neonatal chicks. However, when we performed competition
474 experiments with a mixture of divergent *E. coli* strains originating from fresh and reused
475 litter, *S*. Heidelberg strains emerged with newly acquired antibiotic resistance genes. This
476 result suggests that competition for space and nutrients between closely related species
477 that differ in virulence and resistome can lead to a negative outcome i.e., the development
478 of new multidrug resistant pathogenic strains. Thus, identifying gut conditions that

479 maintains an abundance of beneficial microbes while limiting such “adverse” competition
480 warrants further study.

481 Materials and Methods

482 The details of the methods used for preparing S. Heidelberg (SH) inocula, challenging
483 neonatal chicks, bacterial and DNA analyses, whole genome, and metagenome
484 sequencing and bioinformatics have been described before for neonatal chicks raised on
485 fresh pine shavings (7). Therefore, detailed methods are only provided for experiments
486 involving reused litter.

487 **SH inoculum preparation.** The SH strain was made resistant to 200 ppm of nalidixic
488 acid (nal^R) for selective enumeration. The inoculum was grown overnight in poultry litter
489 extract, centrifuged, and resuspended in 1X phosphate buffered saline (PBS). The
490 resuspended cells were used as inocula. The complete genome of the ancestor to SH-
491 2813nal^R is available under GenBank accession number : CP066851.

492 **Challenging broiler chicks with SH** Two hundred one-day-old Cobb 500 broiler chicks
493 were either uninoculated, gavaged or cloacally inoculated with ~10^6 colony forming units
494 (CFU) of SH-2813nal^R. We included a seeder-bird colonization method, whereby five
495 chicks were gavaged and mingled with twenty uninoculated chicks. Afterwards, chicks
496 were placed in floor pens at a stocking density of 0.65 m^2/chick on fresh pine shavings (n
497 =100) or reused litter (n =100). The reused litter was previously used to raise three flocks
498 of broiler chicken’s antibiotic-free under simulated commercial poultry production
499 conditions and was top dressed with 0.5 cm of fresh pine shavings before the placement
500 of each flock. Broiler chicks on fresh (FL) and reused litter (RL) were housed separately.

501 Broiler chicks were raised for 14 days on antibiotic-free starter diet and water. At 14
502 days, forty-five chicks from FL and RL (ten chicks from gavaved, cloacal and uninoculated
503 groups and fifteen chickens from the seeder method) were sacrificed to determine the
504 extent of SH colonization in ceca. Additionally, litter samples were collected as grab
505 samples from each pen after chicks were culled. The experiments were performed in April
506 2018. The study was approved by the University of Georgia Office of Animal Care and
507 Use under Animal Use Protocol: A2017 04-028-A2.

508 **Determination of cecal and litter *Salmonella* counts** Ceca were removed from the
509 eviscera of broiler chicks and stomached for 60s after the addition 3X volume to the
510 weight (v/w) of buffered peptone water. Serial dilutions of the stomached cecal slurry were
511 plated onto Brilliant Green Sulfa agar (BGS) (BD Difco, MD, USA) containing 200-ppm
512 nal. Plates were incubated for 24 h at 37°C. After incubation, colonies were counted and
513 used for CFU/g calculation. When no colonies appeared, pre-enriched cecal slurry was
514 streaked onto BGS agar supplemented with nal and incubated overnight. BGS plates
515 were examined for the presence/absence of *Salmonella* colonies after overnight
516 incubation. In addition, thirty grams of litter was processed in duplicates from each pen
517 and serial dilutions were plated and analyzed as described for cecal slurry. Colony counts
518 were reported per gram litter dry weight.

519 **Real-time qPCR.** Quantitative real-time PCR amplification was performed on DNA
520 extracted from 250 mg of cecal slurry and litter using a CFX96 Touch Real-Time PCR
521 Detection System (Bio-Rad Inc., Hercules, CA). Reaction mixtures contained 1X
522 SsoAdvanced Universal SYBR Green Supermix (Bio-Rad Inc., Hercules, CA), 600 nM
523 (each) primers) and 2 µl of DNA (7).

524 **16S rRNA gene sequencing.** The V4 hypervariable region of the 16S rRNA gene was
525 sequenced using the paired-end (250 × 2) method on the Illumina MiSeq platform. The
526 samples were part of a larger sequencing run and processed together with other samples.
527 Thus, detailed sequence processing parameters are described in (7). To avoid bias
528 introduced by spurious amplicon sequence variants (ASVs) or from samples with low
529 sequencing depth, any ASVs with less than 5 reads and samples with less than 5000
530 reads were removed from the dataset before further analysis.

531 Statistical analysis of microbial communities was performed in the R environment
532 using the packages “phyloseq”, “Ampvis2”, and “vegan”. Alpha diversity indices were
533 calculated with a dataset rarefied to the minimum sample size (8740 sequences). After
534 assessing normal distribution by qqplots, histograms, and the Shapiro-Wilk normality test,
535 the not normal distributed groups were compared using the Wilcoxon Signed Rank test.
536 The principal coordinates analysis based on Bray-Curtis distances was calculated with
537 no initial data transformation and ASVs that were not present in more than 0.1% relative
538 abundance in any sample have been removed. All raw FASTQ files for 16S rRNA gene
539 sequences have been deposited under NCBI accession number: PRJNA669215.

540 **Cecal metagenome sequencing** Two hundred and fifty milligrams of cecal slurry from
541 chicks cloacally challenged with SH and raised on fresh (n = 2) or reused litter (n = 2)
542 were used for generating shotgun and Hi-C DNA library. For shotgun library, cecal DNA
543 was extracted with Qiagen DNeasy Power-Soil DNA kit (Hilden, Germany) and Nextera™
544 XT library preparation kit was used to make the library. Hi-C library was made using
545 Phase Genomics (Seattle, WA, USA) ProxiMeta Hi-C Microbiome Kit following the
546 manufacturer's instructions. Libraries were sequenced by Novogene corporation

547 (Sacramento, CA, USA) on the Illumina HiSeq platform using 150bp paired end reads.
548 Two libraries were sequenced per HiSeq flowcell lane resulting in a total of ~111 million
549 shotgun reads, and ~213 million Hi-C reads per sample.

550 Shotgun reads were filtered and trimmed for quality and normalized before assembly
551 was performed with metaSPAdes (57) using default options. Hi-C reads were then aligned
552 to the assembly following the Hi-C kit manufacturer's recommendations
553 (https://phasegenomics.github.io/2019/09/19/hic-alignment-and-qc.html). Metagenome
554 deconvolution was performed with ProxiMeta (58, 59), resulting in the creation of putative
555 genome and genome fragment clusters. Hi-C clusters were assessed for quality using
556 CheckM (59) and assigned taxonomic classifications with Mash v2.1. Quality controlled
557 shotgun reads were additionally classified using Kraken2 (v2.0.8 beta) (30) to create a
558 count profile of the metagenome. To identify the plasmids and ARGs present in
559 metagenome assembled genomes, we used Minimap2 (61) to align assembled
560 metagenome contigs to PlasmidFinder (29) and ResFinder (62) database. For contigs
561 aligned using Minimap, a 75% identity threshold was used for the alignment match,
562 whereas contigs with significant homology (E value < 0.05) were considered contigs of
563 the respective plasmid or ARG using Geneious Prime®.

564 **Functional Pathway Analysis** To assess enrichment of functional pathways, both the
565 shotgun sequences and the Hi-C deconvoluted genomes were utilized for each sample.
566 The shotgun metagenomic sequences were aligned to the Hi-C genomic contigs using
567 the BWA-MEM algorithm as implemented in the Burrows-Wheeler Aligner software
568 (v0.7.17) (63). The Hi-C genomic contigs were then annotated using Prokka (v1.13) (64).
569 For each annotated region on the Hi-C genomic contigs, sequences overlapping the

570 annotated region in the sequence alignments were counted using a custom Python script
571 to produce a count matrix of genes for all samples. Gene counts were normalized by gene
572 length and using total sum scaling normalization to control for differences in sequencing
573 depth (65).

574 Enzyme Commission identifiers (EC ID) were extracted from the Prokka annotations
575 for each gene and used to translate counts for genes into counts for each EC ID. Genes
576 that did not have an annotated EC ID were not included in the analysis. For ambiguous
577 EC IDs (e.g., 3.6.3.-), counts were divided evenly into the lowest-level, non-ambiguous
578 EC IDs that were children of that EC ID. For example, if 3.6.3.- included 3.6.3.1, 3.6.3.2,
579 and 3.6.3.3, then a count of 9 for the ambiguous EC ID 3.6.3.- would result in each of the
580 three children EC IDs having a count of 3. EC IDs were then mapped to KEGG functional
581 pathways according to the KEGG ontology. KEGG pathway XML files were retrieved from
582 the KEGG database via HTTP REST query using a custom R script. For each pathway,
583 the adjacency graph was reconstructed from the KEGG XML files, and connected
584 components were determined using depth-first search (66). Scores were calculated for
585 pathways and connected components for each sample using the following equation:

586 $$\text{Score} = \frac{1}{K}\sum_{k=1}^{K}\frac{x_k - \bar{x}}{\sigma}$$

587 where *K* is the number of nodes in each pathway or connected component, x_k is the
588 integer count for node *k* in that pathway, $\bar{x}$ is the mean of the node counts in that pathway,
589 and σ is the standard deviation of the node counts in that pathway. Positive scores
590 indicate average increased "flux" through the pathway or connected component, while

591 negative scores indicate average decreased "flux." This approach is equivalent to
592 averaging Z-scores for each node in each pathway or connected component. Statistical
593 testing was then performed by comparing scores to the Z-distribution. All codes, database
594 files, and analytic data used for functional pathway analysis are available on GitHub :
595 https://github.com/lakinsm/oladeinde-competitive-exclusion.

596 **Isolation of *E. coli* from the ceca of broiler chicks.** The method used for screening
597 frozen cecal contents has been reported (7). Briefly, two cecal slurry from challenged
598 chicks raised on fresh and reused litter were spread plated onto CHROMagar™ plates
599 supplemented with or without gentamicin (8 ppm) and tetracycline (8 ppm), ampicillin (16
600 ppm) and cefoxitin (16 ppm) (Thermo Fisher, Waltham, MA). After 24 h incubation, blue
601 green and blue-cream colonies were counted as presumptive *E. coli* and 4 - 5 colonies
602 (n = 27) from each spread plate were picked and restruck for colony purification.

603 After incubation, a colony representing the different morphologies observed was
604 struck on Eosin Methylene Blue (EMB) (Remel Inc., KS, USA) and incubated overnight
605 at 37 ^{o}C. A characteristic green metallic sheen growth on EMB was used to confirm an
606 isolate as *E. coli*. Colonies were preserved in Luria Bertani broth containing glycerol and
607 frozen before they were used further including solid agar competition with SH.

608 **Solid agar competition between SH and *E. coli*.** Four *E. coli* strains
609 (GenBank/Sample accession numbers: CP066836, JAFCXR000000000, CP066839,
610 SAMN17168891) were selected as AR donors and SH-2813nal^{R} (Sample accession
611 number: SAMN17171078) was used as the recipient (see Fig. 4a for experimental
612 design). Four colonies from SH-2813nal^{R} and one colony from each *E. coli* donor strain

613 (~10^8 CFU in a colony) were selected from overnight cultures grown on sheep blood
614 agar (Remel Inc, San Diego, CA) and resuspended in 1.7 ml microcentrifuge tubes
615 containing 900 µl of 1× PBS. The four SH and *E. coli* colonies were resuspended in
616 separate microcentrifuge tubes i.e., one tube for SH and one tube for all four *E. coli*.
617 Afterwards, recipient and donor were diluted 10,000- and 100,000-fold, respectively,
618 using 1× PBS. Thereafter, 100 µl from the 1:10,000 recipient dilution was spread onto
619 CHROMagar™ ECC (Paris, France) supplemented with or without 10mM $CaCl_2$ (Sigma-
620 Aldrich, St. Louis, MO), 20mM sodium chloride citrate buffer ($Na_3C_6H_5O$) (Sigma-
621 Aldrich, St. Louis, MO) or 1mM 2-hexadecynoic acid (2-HDA) (MJM chemical LLC,
622 Athens, GA) and incubated for 6 h. For details of 2-HDA preparation, see
623 supplementary methods (https://datadryad.org/stash/downloads/file_stream/1003254).
624 Following incubation, 100 µl from the 1:100,000 donor dilution was spread onto the
625 recipient bacterial lawn and incubation continued overnight (n = 3 CHROMagar™ plates
626 per treatment).
627 After incubation, two areas of equal sizes (~0.3 cm^2) were excised from each
628 CHROMagar™ plate and transferred to 900 µl of 1× PBS. Vigorous shaking was done at
629 1,800 rpm with a Fastprep-96 bead beater (MP Biomedicals, Solon, Ohio) for 1 min to
630 suspend the cells from the agar plug. Serial dilutions were then spread onto BGS agar
631 and CHROMagar™ supplemented with or without gentamicin (gen) (16 ppm) or amp (8
632 ppm). Experiments were performed twice, and colonies were counted 18 - 48 h after
633 incubation using a calibrated automated ProtoCOL 3 HD colony counter (Synoptics Inc,
634 MD, USA). Additionally, three SH colonies per replicate were selected from BGS agar
635 plates supplemented with either gen or amp for antibiotic susceptibility testing.

636 **DNA extraction from agar plug lysate** We modified a rapid method developed for
637 extracting DNA from bacteriophages (66). First, we combined triplicates of the agar plug
638 resuspension from the sodium citrate treated agar i.e., excised agar and 1X PBS (~ 1.2
639 ml) and added 120 µl of 10X DNAse buffer before incubating in a dry water bath at 40°C
640 for 30 min. Afterwards, we passed the resuspended agar through a 0.22 µm syringe filter
641 and added 2U of DNase (TURBO DNA-free™ Kit, Thermo Fisher) to the lysate recovered.
642 The DNAse-treated lysate was incubated at 37 ^{o}C for 30 min before the DNase was
643 inactivated with 10 µl of 50 mM EDTA (Sigma-Aldrich, St. Louis, MO).

644 Next, we used a 30kDa Amicon® Ultra-15 centrifugal filter unit (Thermo Fisher) to
645 concentrate the lysate for 5 min at 4,000 x *g* in a swing bucket centrifuge (Eppendorf ;
646 model 5804 R, Hamburg, Germany) . We added 10 µl of 10% sodium dodecyl sulfate
647 solution (Media Tech Inc., VA, USA) and 5 µl of proteinase K (Thermo Fisher) to the
648 concentrated lysate, followed by incubation at 55 ^{o}C for 30 min. Afterwards, lysate DNA
649 was incubated at 70 ^{o}C for 10 min to inactivate proteinase K and reconcentrated in an
650 Eppendorf vacufuge plus concentrator (Thermo Fisher) at 30 °C. Pelleted DNA was
651 reconstituted in 10 µl 1× Tris-EDTA buffer (10 mM Tris-HCL, 1 mM EDTA, pH 7.5), and
652 purified with Zymogen PCR inhibitor removal kit (Zymo Research Corp., CA, USA) as per
653 the manufacturer's instructions. DNA was used for making Nextera XT (Illumina, Inc., CA,
654 USA) libraries in duplicates and sequencing was performed on an Illumina MiSeq platform
655 with 150 paired end reads.).

656 **Antibiotic resistance phenotype determination**. Antimicrobial susceptibility testing
657 (AST) was done on SH and *E. coli* isolates by following the National Antimicrobial
658 Resistance Monitoring System (NARMS) protocol for Gram-Negative bacteria. Results

659 were interpreted according to clinical and laboratory standards institute guidelines and
660 breakpoints established by NARMS. For presumptive SH recombinants selected from
661 mating experiments, we screened sixty colonies on BGS agar supplemented with 8 ppm
662 amp or 16 ppm gen before forty-eight isolates were selected for AST using the NARMS
663 protocol.

664 **Whole genome sequencing and analyses.** DNA was extracted and purified from
665 bacterial colonies using FastDNA spin Kit (MpBio) and Illumina short read sequencing
666 was performed on DNA extracted. Libraries were prepared using either Nextera™ XT or
667 Nextera™ DNA Flex library preparation kits (Illumina, Inc., CA, USA) following the
668 manufacturers protocol. Libraries were sequenced on the Illumina MiSeq platform with
669 150 or 250-bp paired end reads. Additionally, two SH and two *E. coli* isolates were
670 selected for long read sequencing using Sequel II System (PacBio Biosciences Inc., CA,
671 USA). Preparation and sequencing of long read libraries were done by sequencing core
672 centers of University of Georgia and Colorado State University. The method used for read
673 quality control and demultiplexing has been reported (7).

674 Genome assembly, resistome characterization, and quality assessment of assemblies
675 was done using Reads2Resistome pipeline v.1.1.1 (68). We assembled bacterial
676 genomes using either Illumina reads only or Illumina and PacBio reads (Supplementary
677 File 7). Genome annotation was done using Prokka (64), Rapid Annotation using
678 Subsystem Technology (RAST) (69) and BlastKOALA (70). We subtyped the *E. coli*
679 strains using ClermonTyping (71) and Multi-Locus Sequence Typing (MLST) (72),
680 whereas S. Heidelberg was subtyped using cgMLSTFinder v. 1.1 (73). For plasmid typing,
681 we used plasmid MLST (29). To identify prophages, we used PHAST(74).

682 ProgressiveMAUVE v. 1.1.1 (75) and MAFFT v. 1.4.0 (76) implemented in Geneious
683 Prime® v 2020.0.1 were used to align and compare sequences. Roary (77) was used for
684 pan genome analysis and phylogenetic trees were reconstructed using the maximum
685 likelihood (ML) method implemented in RAxML-NG v 1.0.0 (78). IslandViewer (79) was
686 used to predict genomic islands. BLAST database of the bacterial genomes sequenced
687 in this study was made using Geneious Prime®.

688 **SNP and Indel identification** Illumina reads were used to determine single nucleotide
689 polymorphisms (SNPs) and indels present in SH isolates. Alignment of raw FASTQ reads
690 to the genome of SH-ancestor was done using Burrows-Wheeler Aligner (BWA) (63) and
691 SNPs/indels were called using Genome Analysis Toolkit (80). Variant call format (VCF)
692 files of SNPs/Indels are available in Dryad Digital
693 Repository: https://doi.org/10.5061/dryad.c866t1g6c. BlastKOALA was used to identify
694 KEGG (Kyoto Encyclopedia of Genes and Genomes) pathways that sequenced genomes
695 or proteins are capable of. For other bioinformatic analyses performed including read
696 coverage determination through FASTQ alignment and CRISPR array identification, see
697 supplementary methods (Supplementary materials and methods). All raw FASTQ reads
698 for sequenced bacterial genomes and agar lysate are publicly available under NCBI
699 accession numbers: PRJNA683658, PRJNA684578 and PRJNA684580.

700 **Statistical analyses.** Continuous variables did not meet the assumption of a normal
701 distribution; therefore, non-parametric testing for direct comparisons was performed using
702 Wilcoxon rank sum and signed rank tests, and the Kruskal-Wallis rank sum test was used
703 for one-way analysis of variance tests. Furthermore, continuous variables were log-

704 transformed before any statistical tests were performed. Statistical analyses were
705 performed using R (v 3.4.1).

706 **Data availability.** All raw short and long FASTQ reads are publicly available under NCBI
707 accession numbers: PRJNA683658, PRJNA684578 and PRJNA684580. Shotgun and
708 Hi-C reads are publicly available under NCBI accession number: PRJNA688069 and 16S
709 rRNA gene sequences under NCBI accession number: PRJNA669215. Complete
710 genomes for *E. coli* strain Ec-RL-1X is available under GenBank accession number:
711 CP066839. Variant call format (VCF) files of identified SNPs/indels and the Linux/Unix
712 shell script used have been deposited in Dryad Digital Repository:
713 https://doi.org/10.5061/dryad.c866t1g6c.

714 **Ethics statement**. All animal experiments were approved by the University of Georgia
715 Office of Animal Care and Use under Animal Use Protocol: A2017 04-028-A2.

716 **Acknowledgements**. We are grateful to Marlo Sommers, Carolina Hall, Jeromey
717 Jackson, and Latoya Wiggins for their logistical and technical assistance. We also thank
718 Nikki Shariat for reviewing the manuscript. This work was supported by USDA Agricultural
719 Research Service (Project Number: 6040-32000-010-00-D), non-assistance cooperative
720 agreement (58-6040-6-030) between USDA Agricultural Research Service and University
721 of Georgia, Research Foundation, and research service agreement (58-6040-8-035)
722 between USDA Agricultural Research Service and Colorado State University. B.Z was
723 supported by the competence center. The competence center (FFoQSI) is funded by the
724 Austrian ministries BMVIT, BMDW, and the Austrian provinces Niederoesterreich, Upper
725 Austria and Vienna within the scope of COMET-Competence Centers for Excellent

726 Technologies. The Austrian Research Promotion Agency FFG handle the program
727 COMET.
728 This study was supported in part by resources and technical expertise from the
729 Georgia Advanced Computing Resource Center, a partnership between the University of
730 Georgia's Office of the Vice President for Research and Office of the Vice President for
731 Information Technology. Any opinions expressed in this paper are those of the authors
732 and do not necessarily reflect the official positions and policies of the USDA or the
733 National Science Foundation, and any mention of products or trade names does not
734 constitute recommendation for use. The authors declare no competing commercial
735 interests in relation to the submitted work. USDA is an equal opportunity provider and
736 employer.
737 **Author's contributions.** A.O., Z.A., and K.C. designed the study. A.O., G.Z., D.E.C. and
738 C.R. performed live-broiler chicken studies. M.J.R contributed to the design of the solid
739 agar mating experiment. A.O., J.L., G.Z., and D.C. performed bacteriological analyses,
740 antibiotic susceptibility testing, DNA extraction and qPCR. G.Z. and A.O. performed
741 Illumina whole genome sequencing. A.O. performed cecal shotgun and Hi-C library
742 preparation. T.L. made 16S rRNA gene libraries and sequencing. B.Z. performed 16S
743 rRNA bacterial community analysis and interpretation. A.O., Z.A., M.O.P., J.C.T., S.M.L.,
744 R.W., J.L., and D.C. performed bioinformatic analyses and data curation. A.O., J.L. and
745 D.C. performed solid agar mating experiment. A.O., and B.Z. performed statistical
746 analyses. A.O., Z.A., K.C., N.A.C., B.Z., R.W., M.P., S.M.L., G.Z., and J.L. drafted the
747 manuscript, which was reviewed and edited by all authors. A.O., Z.A., and S.A.A.
748 supervised the study.

749 **Reference:**

750 1. C. J. Von Wintersdorff et al., Dissemination of antimicrobial resistance in microbial
751 ecosystems through horizontal gene transfer. Frontiers in microbiology 7, 173
752 (2016).
753 2. C. Ventola (2015) The antibiotic resistance crisis: part 1: causes and threats. PT
754 40 (4): 277–283.
755 3. F. J. Angulo, N. L. Baker, S. J. Olsen, A. Anderson, T. J. Barrett (2004)
756 Antimicrobial use in agriculture: controlling the transfer of antimicrobial resistance
757 to humans. in Seminars in pediatric infectious diseases (Elsevier), pp 78-85.
758 4. K. L. Tang et al., Restricting the use of antibiotics in food-producing animals and
759 its associations with antibiotic resistance in food-producing animals and human
760 beings: a systematic review and meta-analysis. The Lancet Planetary Health 1,
761 e316-e327 (2017).
762 5. R. Singer, L. Porter (2019) Estimates of On-Farm Antimicrobial Usage in Broiler
763 Chicken and Turkey Production in the United States, 2013-2017. . (Mindwalk
764 Consulting Group, LLC. Falcon Heights, MN, 55113, USA.).
765 6. C. Kirchhelle, Swann Song: Antibiotic Regulation in British Livestock Production
766 (1953-2006). B Hist Med 92, 317-351 (2018).
767 7. A. Oladeinde et al., Gene flux and acid-imposed selection are the main drivers of
768 antimicrobial resistance in broiler chicks infected with Salmonella
769 enterica serovar Heidelberg. bioRxiv 10.1101/2021.02.25.432983,
770 2021.2002.2025.432983 (2021).

771 8. L. Gieraltowski et al., National Outbreak of Multidrug Resistant Salmonella
772 Heidelberg Infections Linked to a Single Poultry Company. PLoS One 11,
773 e0162369 (2016).
774 9. R. Edirmanasinghe et al., A Whole-Genome Sequencing Approach To Study
775 Cefoxitin-Resistant Salmonella enterica Serovar Heidelberg Isolates from Various
776 Sources. Antimicrob Agents Chemother 61 (2017).
777 10. D. Ceccarelli et al., Competitive Exclusion Reduces Transmission and Excretion
778 of Extended-Spectrum-beta-Lactamase-Producing Escherichia coli in Broilers.
779 Appl Environ Microbiol 83 (2017).
780 11. I. Chantziaras et al., The effect of a commercial competitive exclusion product on
781 the selection of enrofloxacin resistance in commensal E. coli in broilers. Avian
782 Pathology 47, 443-454 (2018).
783 12. M. Raffatellu, Learning from bacterial competition in the host to develop
784 antimicrobials. Nature medicine 24, 1097-1103 (2018).
785 13. C. S. Achard et al., Variability of the ability of complex microbial communities to
786 exclude microbes carrying antibiotic resistance genes in rabbits. Frontiers in
787 microbiology 10, 1503 (2019).
788 14. M. Baumgartner, F. Bayer, K. R. Pfrunder-Cardozo, A. Buckling, A. R. Hall,
789 Resident microbial communities inhibit growth and antibiotic-resistance evolution
790 of Escherichia coli in human gut microbiome samples. PLoS Biol 18, e3000465
791 (2020).

792 15. A. Dame-Korevaar et al., Early life supply of competitive exclusion products
793 reduces colonization of extended spectrum beta-lactamase-producing Escherichia
794 coli in broilers. Poultry science 99, 4052-4064 (2020).
795 16. U. Methner, U. Rösler, Efficacy of a competitive exclusion culture against
796 extended-spectrum β-lactamase-producing Escherichia coli strains in broilers
797 using a seeder bird model. BMC veterinary research 16, 1-7 (2020).
798 17. L. Wang, M. Lilburn, Z. Yu, Intestinal Microbiota of Broiler Chickens As Affected by
799 Litter Management Regimens. Front Microbiol 7, 593 (2016).
800 18. A. Figueroa et al., Persistence of low and highly pathogenic avian influenza virus
801 in reused poultry litter, effects of litter amendment use, and composting
802 temperatures. Journal of Applied Poultry Research, 100096 (2020).
803 19. S. Wadud et al., Bacterial and fungal community composition over time in chicken
804 litter with high or low moisture content. British poultry science 53, 561-569 (2012).
805 20. National Farm Animal Care Council. Code of Practice: For the care and handling
806 of hatching eggs, breeders, chickens, and turkeys. Retrieved from
807 https://www.nfacc.ca/codes-of-practice/chickens-turkeys-and-breeders. (2016).
808 21. ADAS UK Ltd. Comparison of the Regulatory Framework and Key Practices in the
809 Poultry Meat Supply Chain in the EU and USA : a study for the association of
810 poultry processors and poultry trade in the EU Countries. (2016) Retrieved from
811 https://www.britishpoultry.org.uk/identity-cms/wp-content/uploads/2018/05/2016-
812 ADAS-EU-US-comparison.pdf.22.
813 22 K. C. Dornelas et al., Chicken bed: a review on reuse, treatment and influence on
814 ambience. Poultry Science (2020).

815 23. E. Muniz, D. Mesa, R. Cuaspa, A. M. Souza, E. Santin, Presence of Salmonella
816 spp. in reused broiler litter. Revista Colombiana de Ciencias Pecuarias 27, 12-17
817 (2014).
818 24. U. S. Yamak, M. Sarica, M. A. Boz, A. Ucar, Effect of reusing litter on broiler
819 performance, foot-pad dermatitis and litter quality in chickens with different growth
820 rates. Kafkas Univ. Vet. Fak. J 22, 85-91 (2016).
821 25. R. Casey, B. Fairchild, M. Lacy (2005) Litter quality and broiler performance. ed C.
822 e. S. Bulletin.
823 26. V. F. Roll, M. A. Dai Pra, A. P. Roll, Research on Salmonella in broiler litter reused
824 for up to 14 consecutive flocks. Poult Sci 90, 2257-2262 (2011).
825 27. J. Zucko et al., Probiotic–friend or foe? Current Opinion in Food Science 32, 45-
826 49 (2020).
827 28. S. Gupta, E. Allen-Vercoe, E. O. Petrof, Fecal microbiota transplantation: in
828 perspective. Therapeutic advances in gastroenterology 9, 229-239 (2016).29.
829 29 A. Carattoli *et al.*, In Silico Detection and Typing of Plasmids using PlasmidFinder
830 and Plasmid Multilocus Sequence Typing. *Antimicrob Agents Ch* **58**, 3895-3903
831 (2014).
832 30. D. E. Wood, J. Lu, B. Langmead, Improved metagenomic analysis with Kraken 2.
833 *Genome biology* **20**, 257 (2019).
834 31. J. Haaber *et al.*, Bacterial viruses enable their host to acquire antibiotic resistance
835 genes from neighbouring cells. *Nature Communications* **7** (2016).
836 32. M. Getino *et al.*, Synthetic Fatty Acids Prevent Plasmid-Mediated Horizontal Gene
837 Transfer. *mBio* **6**, e01032-01015 (2015).

838 33. K. Bohm *et al.*, Genes affecting progression of bacteriophage P22 infection in
839 Salmonella identified by transposon and single gene deletion screens. *Mol*
840 *Microbiol* **108**, 288-305 (2018).
841 34. N.-F. Alikhan, Z. Zhou, M. J. Sergeant, M. Achtman, A genomic overview of the
842 population structure of Salmonella. *PLoS genetics* **14**, e1007261 (2018).
843 35. N. Shariat, C. H. Sandt, M. J. DiMarzio, R. Barrangou, E. G. Dudley, CRISPR-
844 MVLST subtyping of Salmonella enterica subsp. enterica serovars Typhimurium
845 and Heidelberg and application in identifying outbreak isolates. *BMC Microbiol* **13**,
846 254 (2013).
847 36. A. Biswas, J. N. Gagnon, S. J. Brouns, P. C. Fineran, C. M. Brown, CRISPRTarget:
848 bioinformatic prediction and analysis of crRNA targets. *RNA Biol* **10**, 817-827
849 (2013).
850 37. S. Bergstrom, F. P. Lindberg, O. Olsson, S. Normark, Comparison of the
851 overlapping frd and ampC operons of Escherichia coli with the corresponding DNA
852 sequences in other gram-negative bacteria. *J Bacteriol* **155**, 1297-1305 (1983).
853 38. H. M. Jones, R. P. Gunsalus, Regulation of Escherichia coli fumarate reductase
854 (frdABCD) operon expression by respiratory electron acceptors and the fnr gene
855 product. *J Bacteriol* **169**, 3340-3349 (1987).
856 39. J.-S. Kim *et al.*, Fumarate-mediated persistence of Escherichia coli against
857 antibiotics. *Antimicrob Agents Ch* **60**, 2232-2240 (2016).
858 40. R. Nakano *et al.*, CFE-1, a novel plasmid-encoded AmpC beta-lactamase with an
859 ampR gene originating from Citrobacter freundii. *Antimicrob Agents Chemother*
860 **48**, 1151-1158 (2004).

861 41. C. M. Chen, M. Huang, H. J. Wu, M. K. Guo, L. T. Wu, Identification of CFE-2, a
862 new plasmid-encoded AmpC beta-lactamase from a clinical isolate of Citrobacter
863 freundii. *Int J Antimicrob Agents* **52**, 421-424 (2018).
864 42. S. Casjens, P. Weigele, "DNA packaging by bacteriophage P22" in Viral Genome
865 Packaging Machines: Genetics, Structure, and Mechanism. (Springer, 2005), pp.
866 80-88.
867 43. B. A. Mann, J. M. Slauch, Transduction of low-copy number plasmids by
868 bacteriophage P22. *Genetics* **146**, 447-456 (1997).
869 44. L. Rodriguez-Rubio *et al.*, Extensive antimicrobial resistance mobilization via
870 multicopy plasmid encapsidation mediated by temperate phages. *J Antimicrob*
871 *Chemother* **75**, 3173-3180 (2020).
872 45. A. Oladeinde *et al.*, Hotspot mutations and ColE1 plasmids contribute to the fitness
873 of Salmonella Heidelberg in poultry litter. *PLoS One* **13**, e0202286 (2018).
874 46. S. Rao *et al.*, Pathogen-mediated inhibition of anorexia promotes host survival and
875 transmission. *Cell* **168**, 503-516. e512 (2017).
876 47. K. V.-A. Johnson, K. R. Foster, Why does the microbiome affect behaviour? *Nature*
877 *reviews microbiology* **16**, 647-655 (2018).
878 48. S. Khan, K. K. Chousalkar, Salmonella Typhimurium infection disrupts but
879 continuous feeding of Bacillus based probiotic restores gut microbiota in infected
880 hens. *Journal of animal science and biotechnology* **11**, 1-16 (2020).
881 49. Y. Litvak *et al.*, Commensal Enterobacteriaceae Protect against Salmonella
882 Colonization through Oxygen Competition. *Cell Host Microbe* **25**, 128-139 e125
883 (2019).

884 50. K. K. Mon *et al.*, Salmonella enterica serovars Enteritidis infection alters the
885 indigenous microbiota diversity in young layer chicks. *Frontiers in veterinary*
886 *science* **2**, 61 (2015).
887 51. B. Stecher *et al.*, Gut inflammation can boost horizontal gene transfer between
888 pathogenic and commensal Enterobacteriaceae. *Proceedings of the National*
889 *Academy of Sciences* **109**, 1269-1274 (2012).
890 52. A. W. Rogers, R. M. Tsolis, A. J. Bäumler, Salmonella versus the Microbiome.
891 *Microbiol Mol Biol R* **85** (2021).
892 53. G. Casaburi *et al.*, Early-life gut microbiome modulation reduces the abundance of
893 antibiotic-resistant bacteria. *Antimicrobial Resistance & Infection Control* **8**, 1-18
894 (2019).
895 54. Nepal, Suruchi, et al. "An ancient family of mobile genomic islands introducing
896 cephalosporinase and carbapenemase genes in Enterobacteriaceae." Virulence
897 9.1 (2018): 1377-1389.
898 55. S. Meini, C. Tascini, M. Cei, E. Sozio, G. M. Rossolini, AmpC β-lactamase-
899 producing Enterobacterales: what a clinician should know. *Infection* **47**, 363-375
900 (2019).
901 56. F. Maguire, M. A. Rehman, C. Carrillo, M. S. Diarra, R. G. Beiko, Identification of
902 primary antimicrobial resistance drivers in agricultural nontyphoidal Salmonella
903 enterica serovars by using machine learning. *Msystems* **4** (2019).
904 57. S. Nurk, D. Meleshko, A. Korobeynikov, P. A. Pevzner, metaSPAdes: a new
905 versatile metagenomic assembler. *Genome Res* **27**, 824-834 (2017).

906 58. M. O. Press *et al.*, Hi-C deconvolution of a human gut microbiome yields high-
907 quality draft genomes and reveals plasmid-genome interactions. *biorxiv*, 198713
908 (2017).
909 59. R. D. Stewart *et al.*, Assembly of 913 microbial genomes from metagenomic
910 sequencing of the cow rumen. *Nat Commun* **9**, 870 (2018).
911 60. D. H. Parks, M. Imelfort, C. T. Skennerton, P. Hugenholtz, G. W. Tyson, CheckM:
912 assessing the quality of microbial genomes recovered from isolates, single cells,
913 and metagenomes. *Genome Res* **25**, 1043-1055 (2015).
914 61. H. Li, Minimap2: pairwise alignment for nucleotide sequences. *Bioinformatics* **34**,
915 3094-3100 (2018).
916 62. E. Zankari *et al.*, Identification of acquired antimicrobial resistance genes. *J*
917 *Antimicrob Chemother* **67**, 2640-2644 (2012).
918 63. H. Li, R. Durbin, Fast and accurate short read alignment with Burrows-Wheeler
919 transform. *Bioinformatics* **25**, 1754-1760 (2009).
920 64. T. Seemann, Prokka: rapid prokaryotic genome annotation. *Bioinformatics* **30**,
921 2068-2069 (2014).
922 65. J. N. Paulson, O. C. Stine, H. C. Bravo, M. Pop, Differential abundance analysis
923 for microbial marker-gene surveys. *Nature methods* **10**, 1200-1202 (2013).
924 66. G. Csardi, T. Nepusz, The igraph software package for complex network research.
925 *InterJournal, complex systems* **1695**, 1-9 (2006).
926 67. W. Kot, F. K. Vogensen, S. J. Sorensen, L. H. Hansen, DPS - a rapid method for
927 genome sequencing of DNA-containing bacteriophages directly from a single
928 plaque. *J Virol Methods* **196**, 152-156 (2014).

929 68. R. R. Woyda, A. Oladeinde, Z. Abdo, Reads2Resistome: An adaptable and high-
930 throughput whole-genome sequencing pipeline for bacterial resistome
931 characterization. *bioRxiv* 10.1101/2020.05.18.102715, 2020.2005.2018.102715
932 (2020).
933 69. T. Brettin *et al.*, RASTtk: a modular and extensible implementation of the RAST
934 algorithm for building custom annotation pipelines and annotating batches of
935 genomes. *Sci Rep* **5**, 8365 (2015).
936 70. M. Kanehisa, Y. Sato, K. Morishima, BlastKOALA and GhostKOALA: KEGG Tools
937 for Functional Characterization of Genome and Metagenome Sequences. *J Mol*
938 *Biol* **428**, 726-731 (2016).
939 71. J. Beghain, A. Bridier-Nahmias, H. Le Nagard, E. Denamur, O. Clermont,
940 ClermonTyping: an easy-to-use and accurate in silico method for Escherichia
941 genus strain phylotyping. *Microb Genom* **4** (2018).
942 72. M. V. Larsen *et al.*, Multilocus sequence typing of total-genome-sequenced
943 bacteria. *J Clin Microbiol* **50**, 1355-1361 (2012).
944 73. P. T. Clausen, F. M. Aarestrup, O. Lund, Rapid and precise alignment of raw reads
945 against redundant databases with KMA. *BMC bioinformatics* **19**, 1-8 (2018).
946 74. Y. Zhou, Y. Liang, K. H. Lynch, J. J. Dennis, D. S. Wishart, PHAST: a fast phage
947 search tool. *Nucleic Acids Res* **39**, W347-352 (2011).
948 75. A. E. Darling, B. Mau, N. T. Perna, progressiveMauve: multiple genome alignment
949 with gene gain, loss and rearrangement. *PLoS One* **5**, e11147 (2010).
950 76. K. Katoh, D. M. Standley, MAFFT multiple sequence alignment software version
951 7: improvements in performance and usability. *Mol Biol Evol* **30**, 772-780 (2013).

952 77. A. J. Page *et al.*, Roary: rapid large-scale prokaryote pan genome analysis.
953 *Bioinformatics* **31**, 3691-3693 (2015).
954 78. A. M. Kozlov, D. Darriba, T. Flouri, B. Morel, A. Stamatakis, RAxML-NG: a fast,
955 scalable and user-friendly tool for maximum likelihood phylogenetic inference.
956 *Bioinformatics* **35**, 4453-4455 (2019).
957 79. Bertelli, Claire, et al. "IslandViewer 4: expanded prediction of genomic islands for
958 larger-scale datasets." Nucleic acids research 45.W1 (2017): W30-W35.
959 80. A. McKenna *et al.*, The Genome Analysis Toolkit: a MapReduce framework for
960 analyzing next-generation DNA sequencing data. *Genome Res* **20**, 1297-1303
961 (2010).
962
963

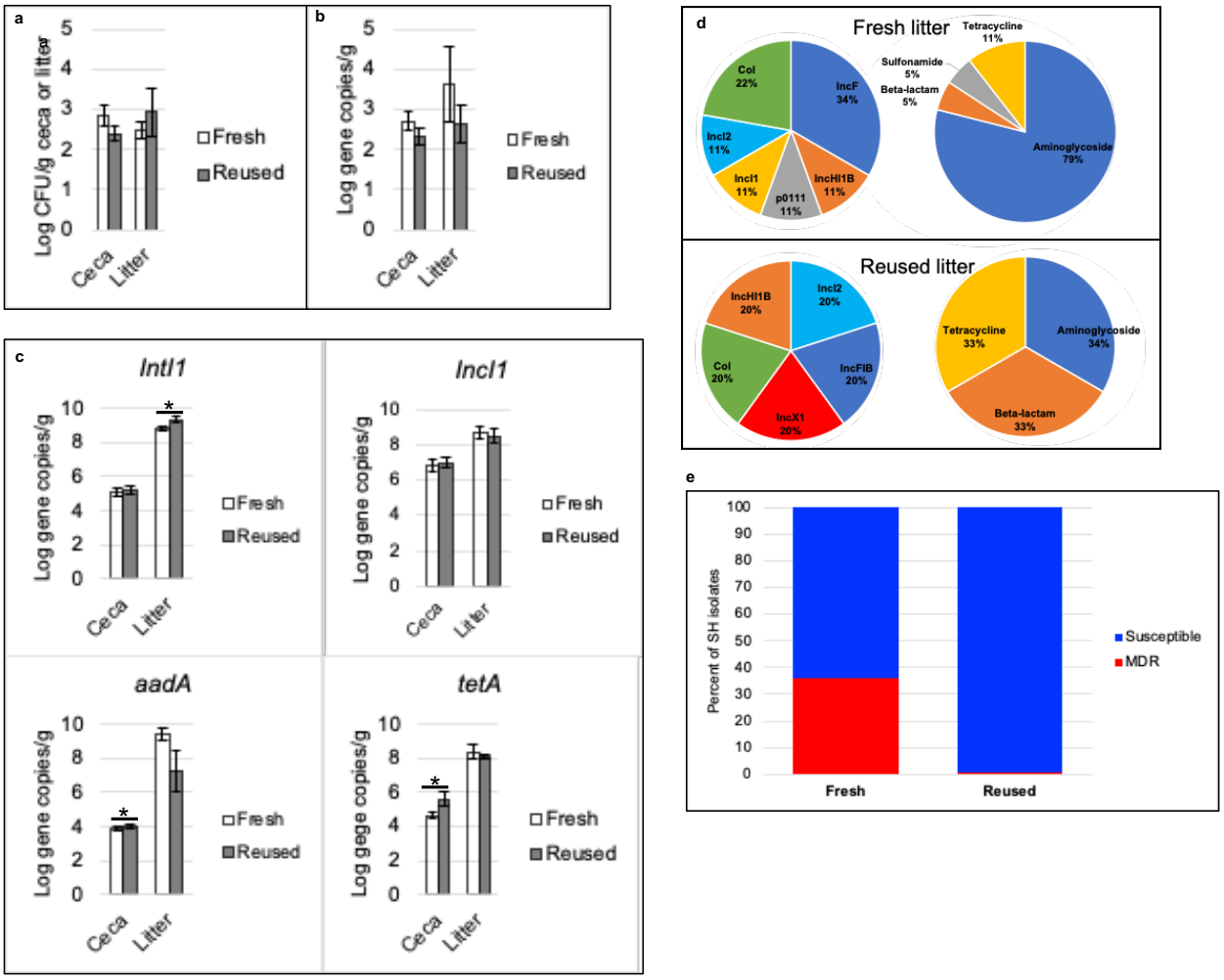

Fig 1. Neonatal chicks raised on reused litter carried lower levels of multidrug resistant *S.* Heidelberg. SH load in the ceca and litter (dry weight of litter) of broiler chicks (n = 70) raised on fresh or reused litter was determined using direct culture method (**a**) and real-time quantitative PCR (reported as gene copies) **(b**). **(c)** Gene copies of IncI1 encoded genes in the ceca (n =70) and litter (n = 12) of neonatal chicks raised on fresh or reused litter. (*P < 0.05 (Kruskal-Wallis test, Error bar = Standard error)). (**d**) Relative number of transferrable Enterobacteriaceae plasmids and ARG's found in the metagenome assembled genomes of chicks raised on fresh (n=2) and reused litter (n =2). **(e**) Percentage of SH isolates in the ceca and litter that acquired multidrug resistance in fresh (n = 158) and reused litter (n = 141).

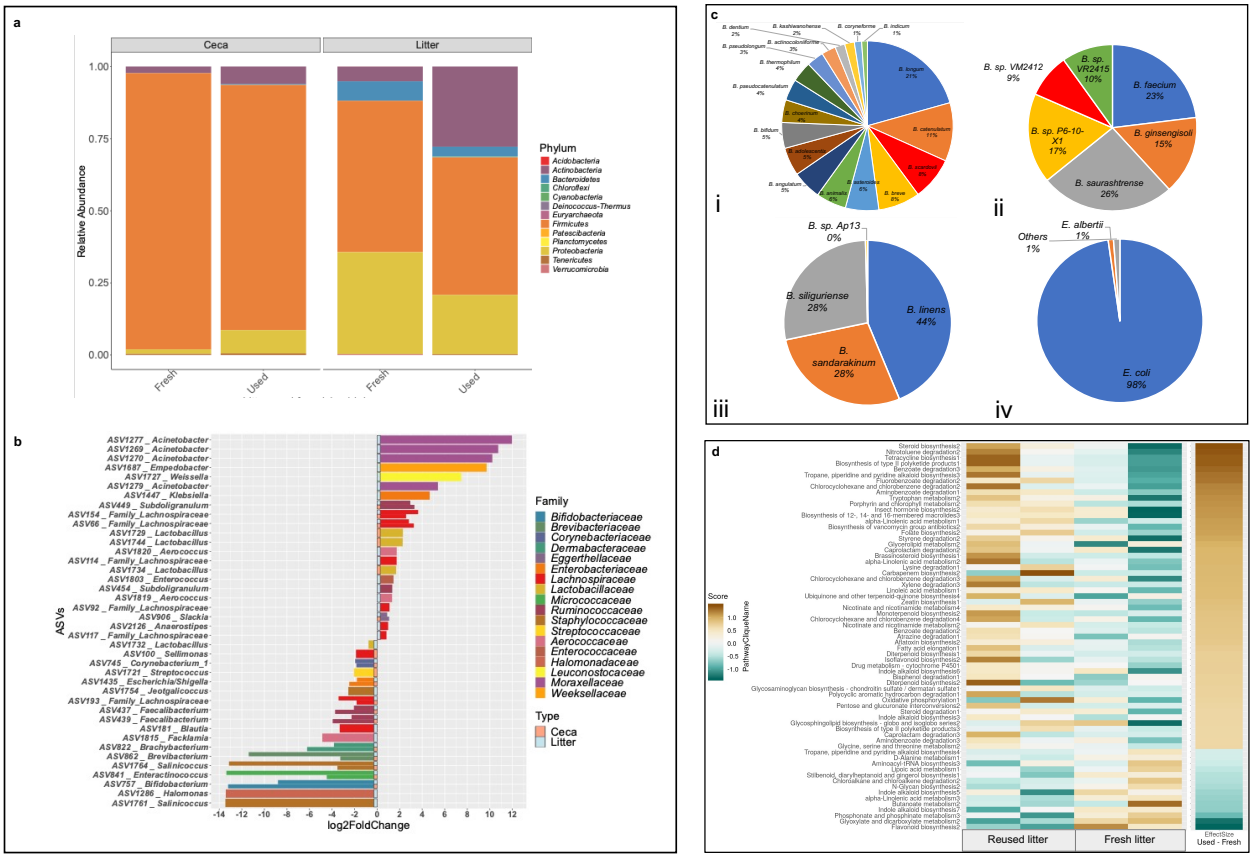

Fig 2. Reused litter is diverse in beneficial bacteria and antimicrobial metabolic pathways. (**a)** Phylum-level classification of 16S rRNA gene sequence reads in ceca and litter grouped by litter type. Data represent average of amplicon sequence variant (ASV) counts from replicate libraries for each category. (**b)** Plots of amplicon sequence variants (ASVs) that were significantly differentially abundant in the ceca and litter of chicks raised on fresh compared to reused litter ($p_{adj} < 0.05$). Significant ASVs are plotted individually and colored according to their family-level classification. **(c)** Relative abundance of bacterial species found using cecal metagenome shot gun reads to be associated with 16S rRNA amplicon sequence variants of the genera (i) *Bifidobacterium* (ii) *Brachybacterium* (iii) *Brevibacterium* and (iv) *Escherichia*. **(d)** Functional metabolic pathways that were enriched in the ceca of chicks from fresh compared to reused litter using metagenome assembled genomes. For a pathway or connected component within a pathway (clique), the flux is the Z-score deviation from the mean taken across all samples (n = 4). Pathway scores for each connected component are shown for each sample, and the difference of used minus fresh litter scores is shown on the right column labelled “effect size. Higher effect size indicates upregulation of the pathway in the reused litter, while lower effect size indicates upregulation in fresh litter.

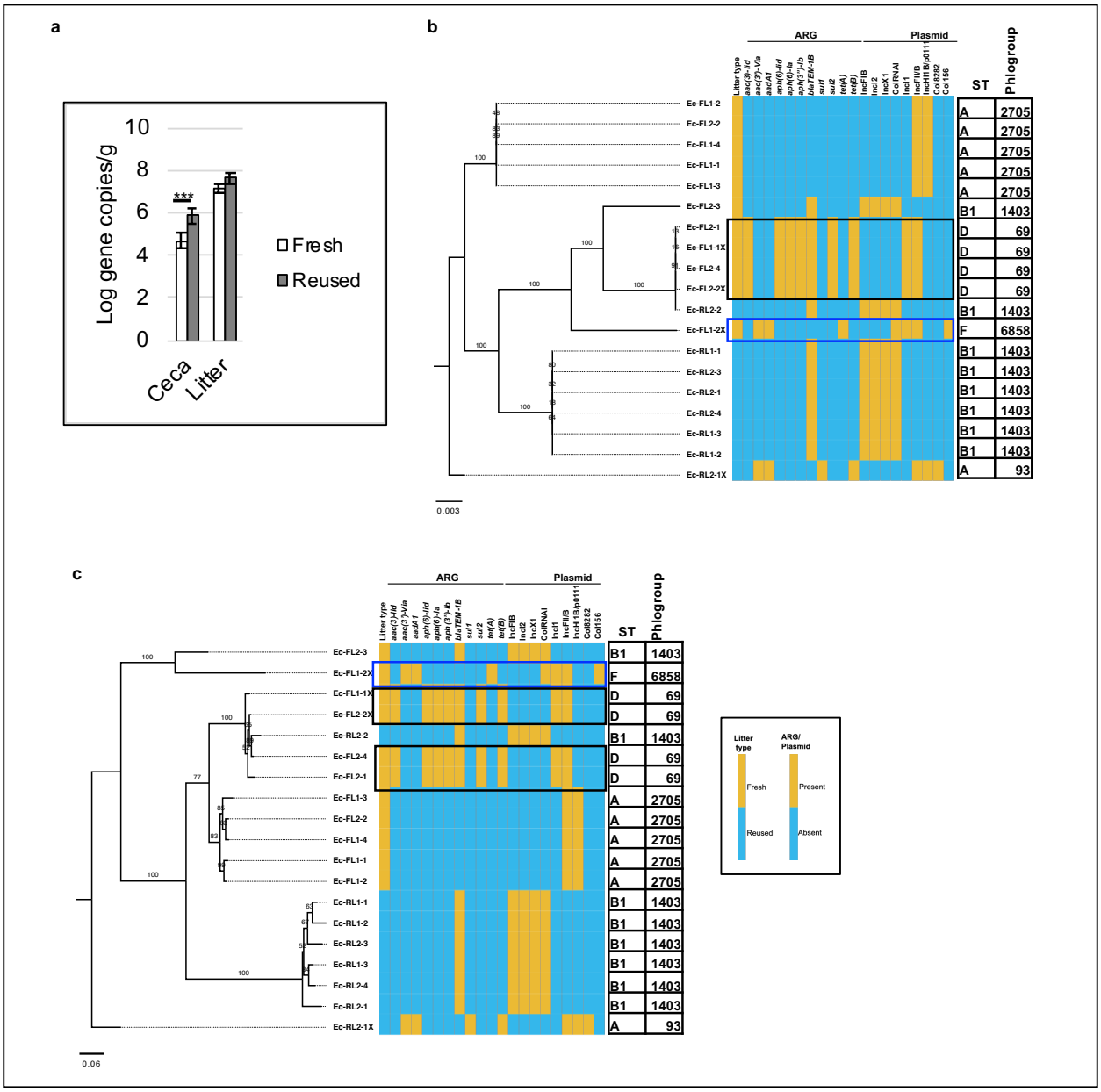

Fig 3. *Escherichia coli* from fresh litter was the main reservoir of transferable ARG. a) *E. coli* load in the ceca and litter (dry weight of litter) of broiler chicks of raised on fresh or reused litter was determined using direct culture method (**a**) and real-time quantitative PCR (reported as gene copies). Primers targeting the housekeeping gene (*gapA*) was used for *E. coli* quantification, (**b and c)** Whole genome sequencing were performed on *E. coli* strains (n =19) recovered from the ceca of four broiler chicks challenged with SH and raised on fresh (FL) or reused litter (RL). Maximum likelihood tree reconstructed using the core (**b)** and accessory **(c**) genes of the *E. coli* strains. GTR model of nucleotide substitution and GAMMA model of rate heterogeneity was used for sequence evolution prediction. Numbers shown next to the branches represent the percentage of replicate trees where associated isolates cluster together based on ~100 bootstrap replicates. Tree was rooted with Ec-RL2-1X. (Note: ST – Multi locus Sequence Type). Blue rectangular box shows the *E. coli* donor strain carrying IncI1-pMLST26 that was acquired by SH. Black box denotes strains of *E. coli* where the ARG's were encoded on the chromosome.

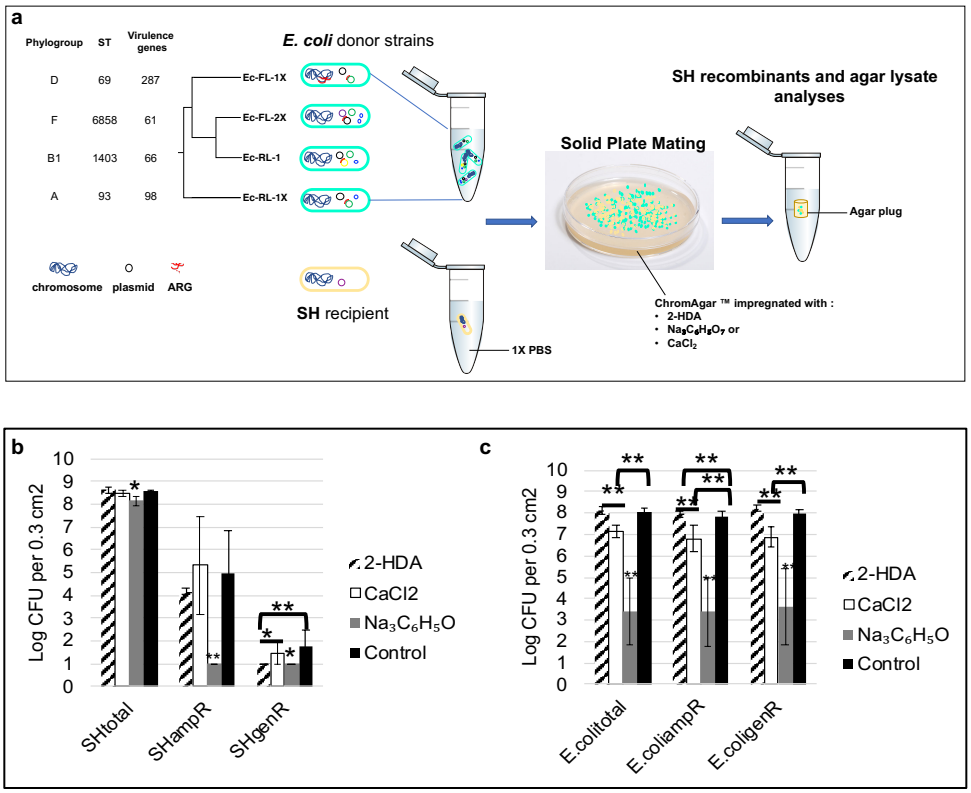

Fig 4. **Competition gave rise to ampicillin and gentamicin resistance *S*. Heidelberg population**. **(a)** Experimental design used for solid agar competition experiment between SH and *E. coli*. SH-2813nal^R recipient was spread plated onto CHROMagar™ supplemented with or without 2-Hexadecynoic acid (2-HDA), sodium citrate or calcium chloride and incubated for 6 h. Afterwards, four *E. coli* strains were spread plated onto SH -2813nal^R bacterial lawn and incubation continued for another 20 – 24 h. Thereafter, agar plugs were used for bacterial enumeration and agar lysate extraction. **(b and c)** SH recombinants (**b**) and *E. coli* donor population (**c**) in agar plugs was determined on Brilliant Green Sulfur agar and CHROMagar™ supplemented with or without gentamicin (16 ppm) or ampicillin (8 ppm) (total = bacterial population on agar with no antibiotic, amp^R/gen^R – bacterial population on agar supplemented with ampicillin or gentamicin). Colonies were counted using a calibrated automatic colony counter (ProtoCOL 3- Synoptics Ltd) (*P < 0.05, **P < 0.01 (Kruskal-Wallis test, multiple comparison correction; Error bar = Standard deviation)).

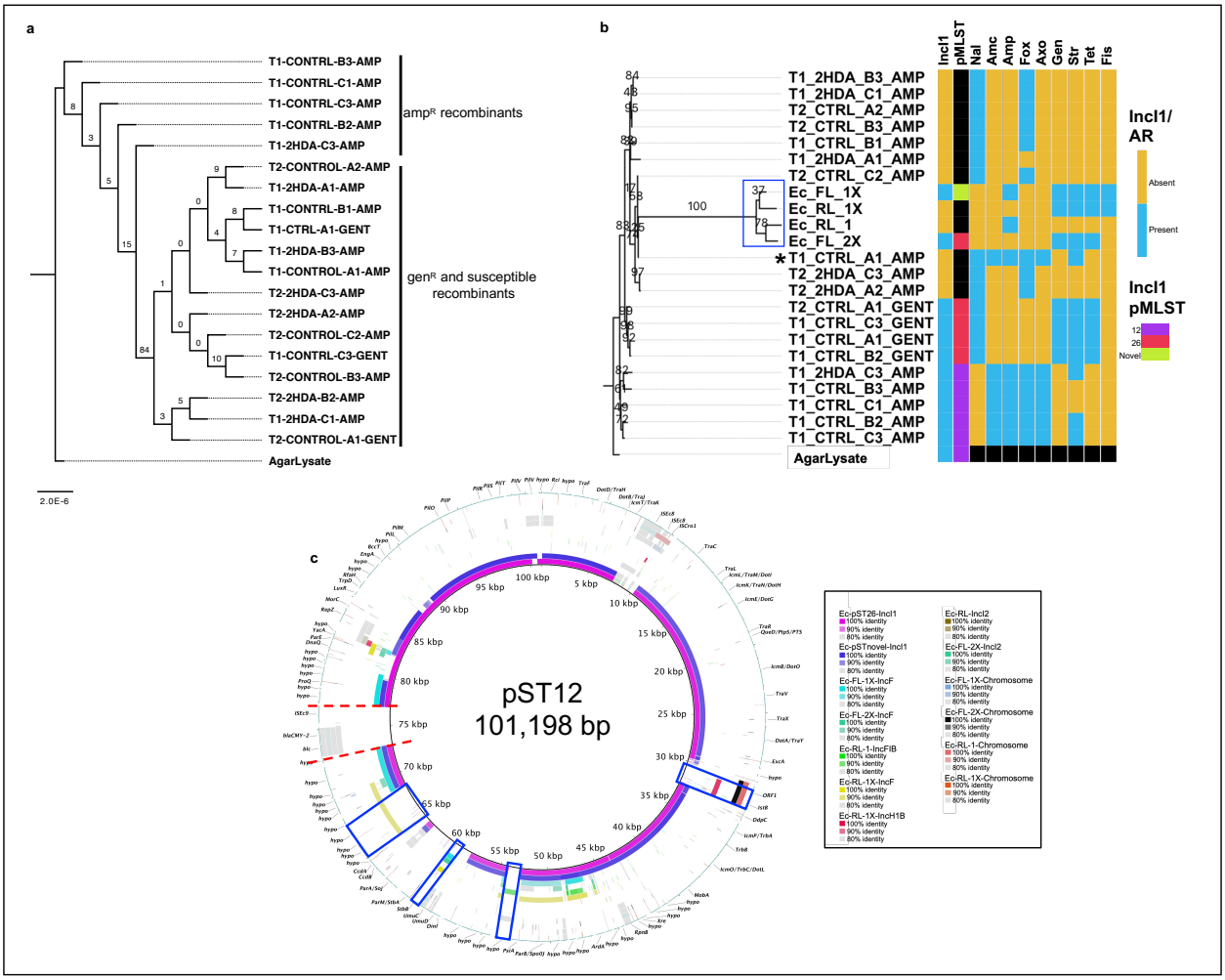

Fig 5. Multidrug resistance strains of *S.* Heidelberg evolved through genetic recombination with *E. coli*. (**a and b**) Maximum likelihood tree reconstructed using SNPs/Indel (**a**) found on the chromosome of SH recombinants and agar lysate, and the accessory genes they carried (**b**) GTR and JC model of nucleotide substitution was used for SNP and accessory gene tree, respectively and the GAMMA model of rate heterogeneity was used for sequence evolution prediction. Rectangular blue box is to highlight the four *E. coli* donor strains used for mating and asterisk denotes one β-lactam resistant SH recombinant that lost the bla_{CMY-2}. genetic determinants prior to sequencing. (Legend: Nal – nalidixic acid, Gen – gentamicin, Str – streptomycin, Tet – tetracycline, Fis – sulfisoxazole, Amc - amoxicillin-clavulanic acid, Amp – ampicillin, Fox – cefoxitin, Axo – Ceftriaxone, pMLST – plasmid multilocus sequence type). Numbers shown next to the branches represent the percentage of replicate trees where associated isolates cluster together based on ~100 bootstrap replicate. Tree was rooted with agar lysate. (**c**) BLASTn alignment of chromosome and all plasmids harbored by *E. coli* donors except IncX1 and Col-like plasmids. The IncI1 plasmid encoding bla_{CMY-2} (pST12 -102 kb) found in amp^R recombinants was used as the reference genome. Red dashed vertical lines highlights pST12 region encoding the bla_{CMY-2} operon whereas blue rectangular box highlights regions encoded by IncFII/FIB and IncH1B plasmids.

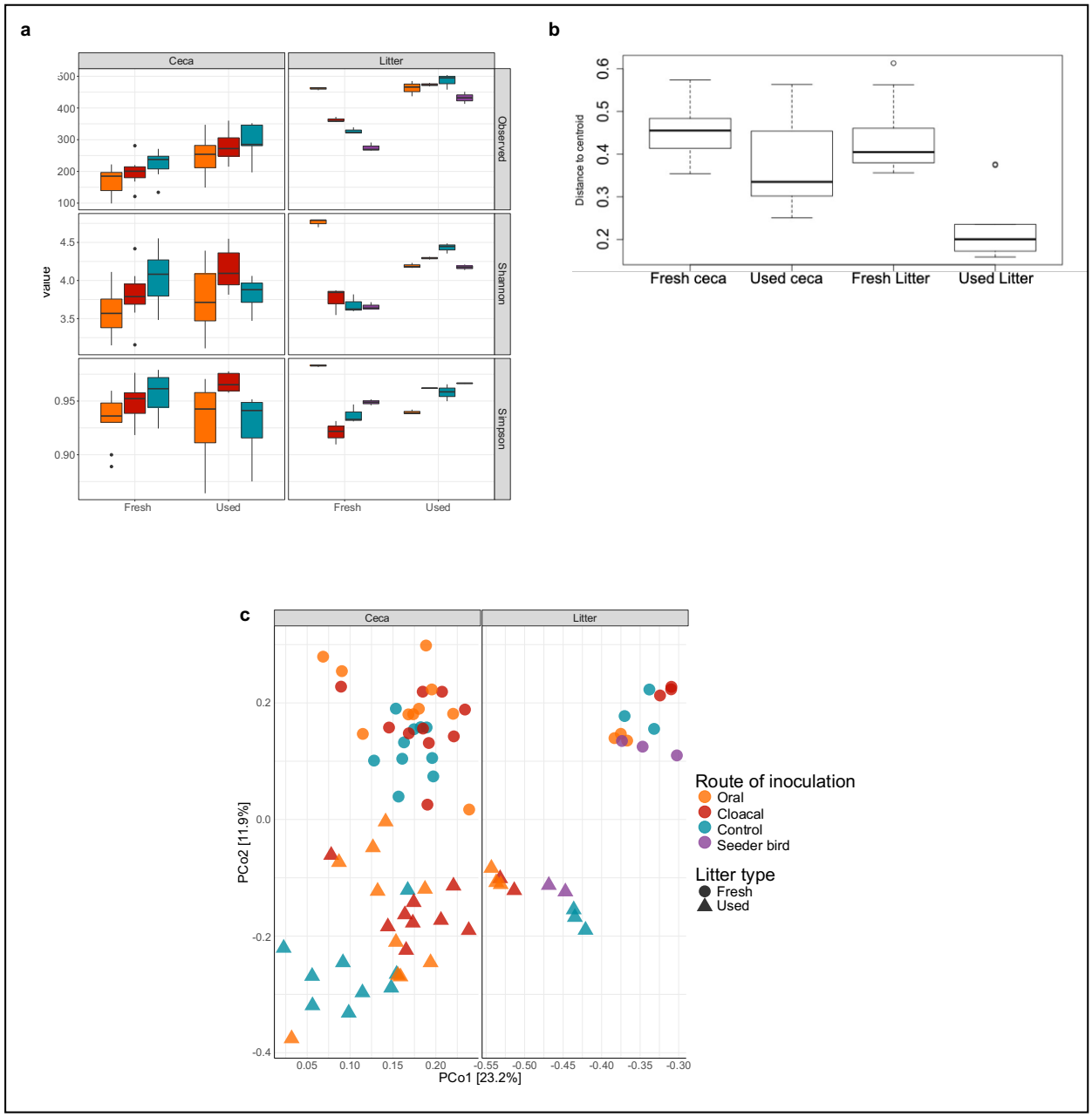

Supplementary Fig. 1. **Reused litter harbored a more uniform bacterial community with higher diversity** (**a**) Average alpha diversity indices of ceca and litter samples grouped by litter type and route of SH challenge. Boxes indicate the interquartile range (75th to 25th) of the data. Whiskers extend to the most extreme value within 1.5 * interquartile range and dots represent outliers beyond that range. (**b**) Variability in bacterial community structure (assessed by analysis of β dispersion, a metric of variability) between fresh and reused litter (**c**) Principal coordinates analysis of Bray-Curtis distances based on 16S rRNA gene libraries. Each point represents values from individual libraries with shapes denoting litter type and colors expressing the route of SH challenge for respective samples.

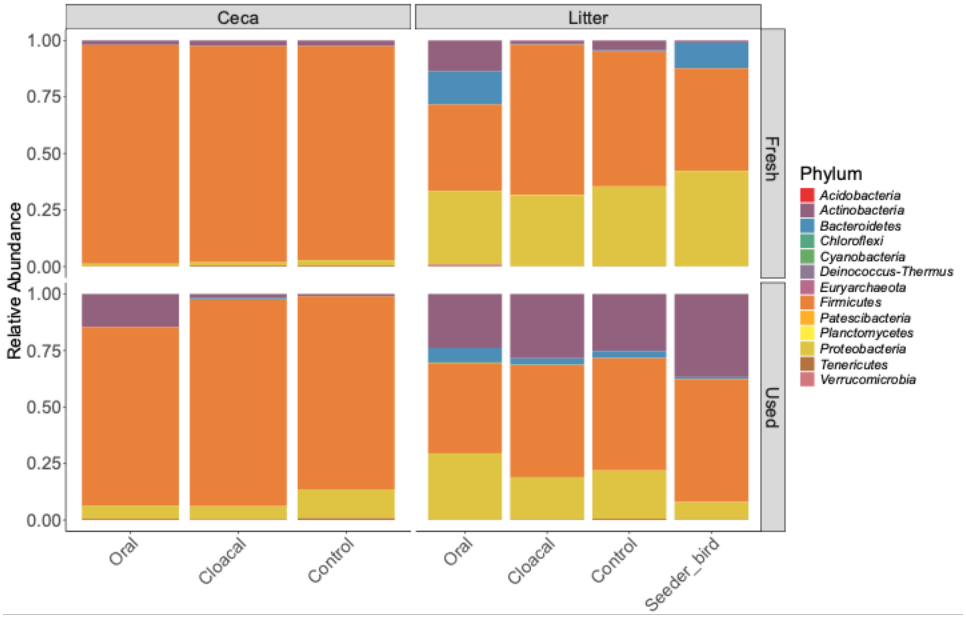

Supplementary Fig. 2. Phylum-level classification of 16S rRNA gene sequence reads in ceca and litter grouped by litter type and route of SH challenge. Data represent average of amplicon sequence variant counts from replicate libraries for each category.

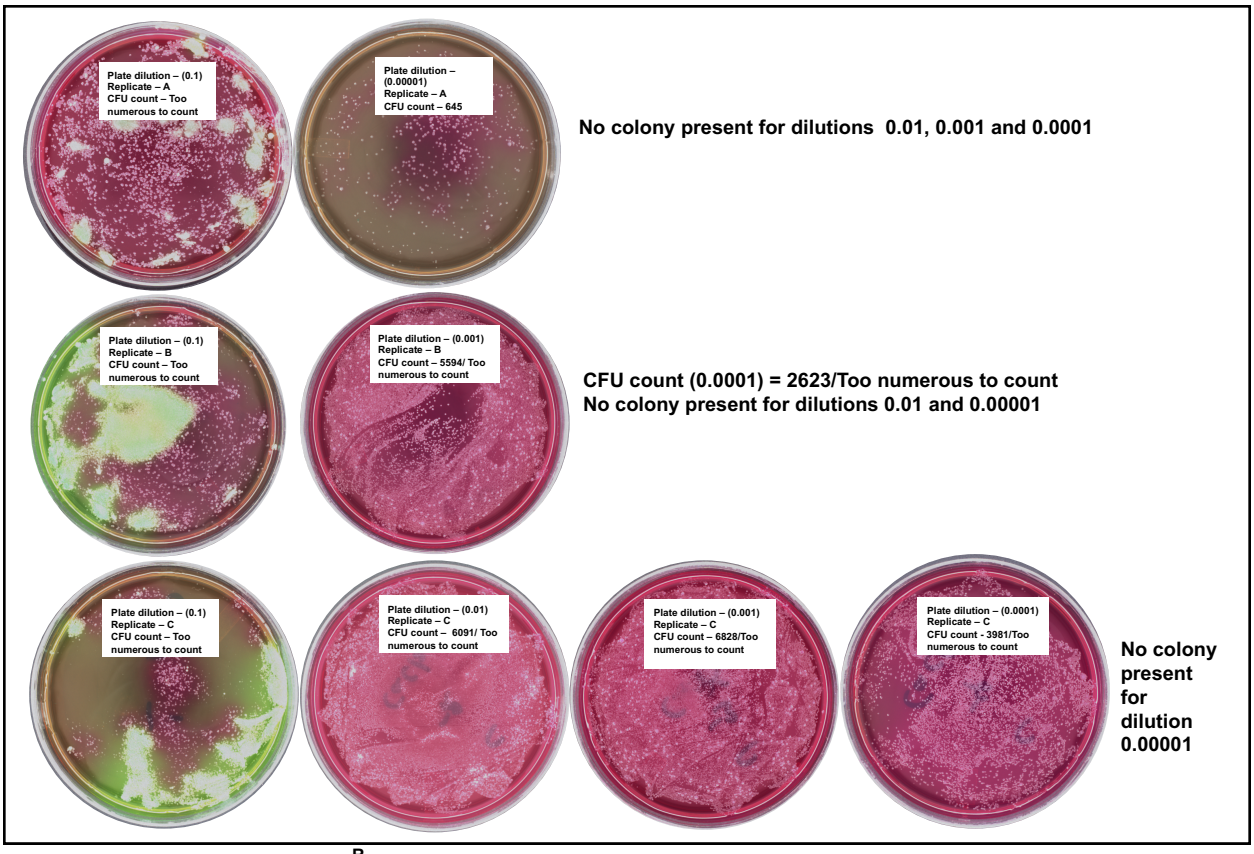

Supplementary Fig. 3. Amp^{R} *S*. Heidelberg recombinants displayed delayed spontaneous growth. SH colony counts after 48 h of incubation on brilliant green sulfur agar supplemented with 8 ppm of ampicillin. Counts were made from serial dilutions of agar plugs excised from the CHROMagar™ used for competition between SH and *E. coli*. Counting of colonies and photograph of plate counted were done using a preconfigured automated colony counter.

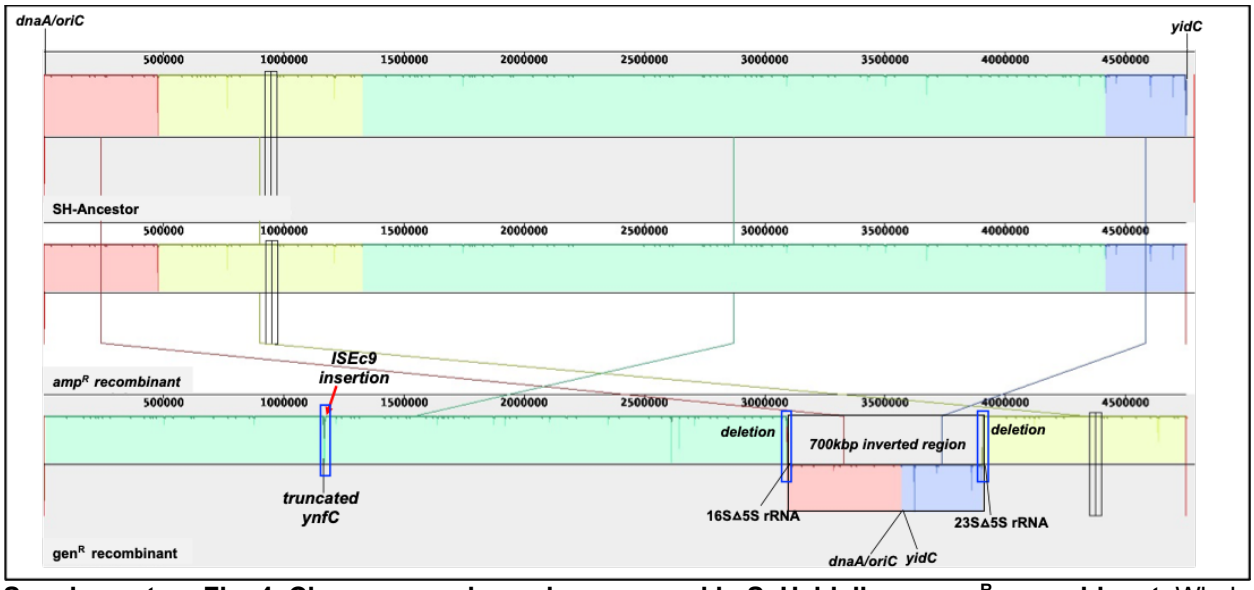

Supplementary Fig. 4. Chromosome inversion occurred in S. Heidelberg amp^R recombinant. Whole genome comparison of amp^R and gen^R recombinants against the chromosome of SH-ancestor. A colored similarity plot is shown for each genome, the height of which is proportional to the level of sequence identity in that region. When the similarity plot points downward it indicates an alignment to the reverse strand of the genome of SH-ancestor i.e., inversion. Segment highlighted with horizontal blue box denotes regions with relevant mutations.

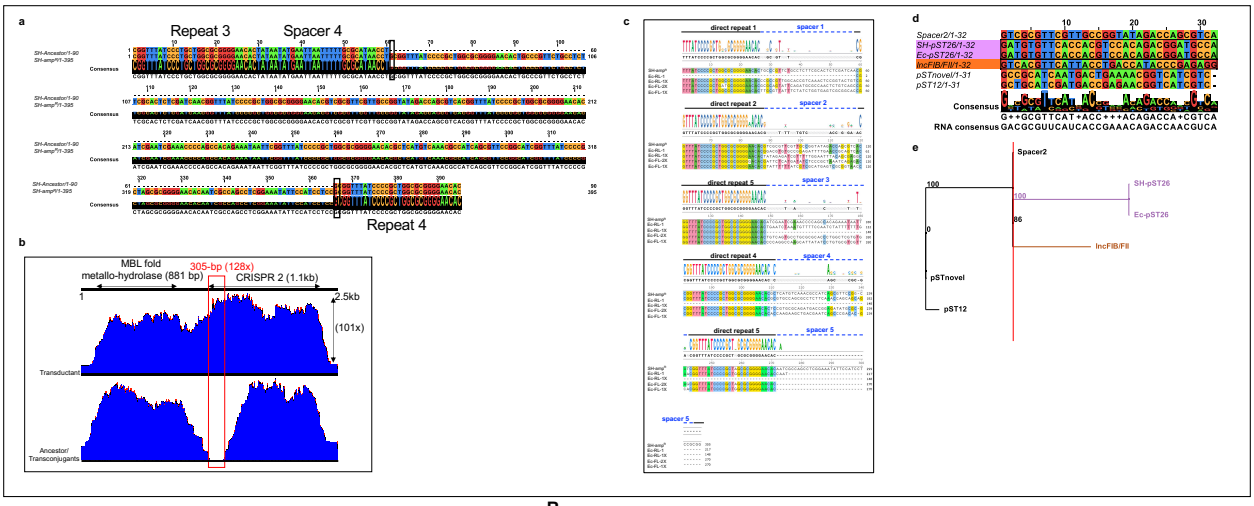

Supplementary Fig. 5. S. Heidelberg amp^R recombinants that acquired IncI1 plasmid encoding *bla*$_{CMY-2}$ adapted new CRISPR spacers. (**a**) Pairwise alignment of CRISPR2 loci (395 of the ~1.1kb CRISPR2 region) of amp^R recombinant and SH-ancestor. The repeat was inserted after spacer 4 and before repeat 4 present in the ancestral CRISPR2. Black rectangular box highlights extra "G" nucleotide that is not part of the CRISPR2 repeat consensus sequence. **(b)** Sequence read coverage (x) of the CRISPR2 loci (~1.1 kb) of a selected amp^R and gen^R recombinant. Red rectangular box shows the extra 305-bp CRISPR repeat present in ampR recombinants. (**c)** DNA alignment of the new CRISPR array (305 bp) added to CRISPR2 of SH amp^R recombinant and identical CRISPR regions in *E. coli* donor strains used for competition experiment. The numbering of the CRISPR repeat and spacer are arbitrary and should not be interpreted to mean the order of acquisition. **(d)** Alignment of identical DNA sequences in spacer 2 of the new CRISPR array of SH amp^R recombinant and *sopB* gene (plasmid partition protein) of IncFIB/FII and IncI1 plasmids (pST26, pSTnovel and pST12). RNA consensus sequence was determined using RNAifold implemented in Jalview v. 2.11.1.3. (**e)** A maximum likelihood tree reconstructed from the aligned DNA sequences in "d". Taxa text color in tree matches color of sequence name in DNA sequence alignment.

1192 **Supplementary Fig. 1**. **Reused litter harbored a more uniform bacterial community with higher**
1193 **diversity** (**a**) Average alpha diversity indices of ceca and litter samples grouped by litter type and route of
1194 SH challenge. Boxes indicate the interquartile range (75th to 25th) of the data. Whiskers extend to the
1195 most extreme value within 1.5 * interquartile range and dots represent outliers beyond that range. (**b**)
1196 Variability in bacterial community structure (assessed by analysis of β dispersion, a metric of variability)
1197 between fresh and reused litter (**c)** Principal coordinates analysis of Bray-Curtis distances based on 16S
1198 rRNA gene libraries. Each point represents values from individual libraries with shapes denoting litter type
1199 and colors expressing the route of SH challenge for respective samples.
1200
1201 **Supplementary Fig. 2.** Phylum-level classification of 16S rRNA gene sequence reads in ceca and litter
1202 grouped by litter type and route of SH challenge. Data represent average of amplicon sequence variant
1203 counts from replicate libraries for each category.
1204
1205 **Supplementary Fig. 3. Amp^R *S*. Heidelberg recombinants displayed delayed spontaneous growth.**
1206 SH colony counts after 48 h of incubation on brilliant green sulfur agar supplemented with 8 ppm of
1207 ampicillin. Counts were made from serial dilutions of agar plugs excised from the CHROMagar™ used for
1208 competition between SH and *E. coli*. Counting of colonies and photograph of plate counted were done using
1209 a preconfigured automated colony counter.
1210
1211 **Supplementary Fig. 4. Chromosome inversion occurred in S. Heidelberg amp^R recombinant**. Whole
1212 genome comparison of amp^R and gen^R recombinants against the chromosome of SH-ancestor. A colored
1213 similarity plot is shown for each genome, the height of which is proportional to the level of sequence identity
1214 in that region. When the similarity plot points downward it indicates an alignment to the reverse strand of
1215 the genome of SH-ancestor i.e., inversion. Segment highlighted with horizontal blue box denotes regions
1216 with relevant mutations.
1217
1218 **Supplementary Fig. 5. S. Heidelberg amp^R recombinants that acquired IncI1 plasmid encoding**
1219 ***bla$_{CMY-2}$* adapted new CRISPR spacers.** (**a**) Pairwise alignment of CRISPR2 loci (395 of the ~1.1kb
1220 CRISPR2 region) of amp^R recombinant and SH-ancestor. The repeat was inserted after spacer 4 and before
1221 repeat 4 present in the ancestral CRISPR2. Black rectangular box highlights extra "G" nucleotide that is not
1222 part of the CRISPR2 repeat consensus sequence. **(b)** Sequence read coverage (x) of the CRISPR2 loci
1223 (~1.1 kb) of a selected amp^R and gen^R recombinant. Red rectangular box shows the extra 305-bp CRISPR
1224 repeat present in ampR recombinants. (**c)** DNA alignment of the new CRISPR array (305 bp) added to
1225 CRISPR2 of SH amp^R recombinant and identical CRISPR regions in *E. coli* donor strains used for
1226 competition experiment. The numbering of the CRISPR repeat and spacer are arbitrary and should not be
1227 interpreted to mean the order of acquisition. **(d)** Alignment of identical DNA sequences in spacer 2 of the
1228 new CRISPR array of SH amp^R recombinant and *sopB* gene (plasmid partition protein) of IncFIB/FII and
1229 IncI1 plasmids (pST26, pSTnovel and pST12). RNA consensus sequence was determined using RNAifold
1230 implemented in Jalview v. 2.11.1.3. (**e)** A maximum likelihood tree reconstructed from the aligned DNA
1231 sequences in "d". Taxa text color in tree matches color of sequence name in DNA sequence alignment.
1232
1233
1234
1235
1236
1237
1238
1239